

# Light-derived additive manufacturing: advances, challenges and prospects

Chaoqian Zhao<sup>1,2,3</sup>, Defu Liu<sup>1,2,3</sup>, Jiawei Zhou<sup>1,2,3</sup>, Yong Hu<sup>1,2,3</sup>, Gang Dong<sup>1,2,3</sup>, Zexin Yu<sup>1,2,3</sup>, Liang Wang<sup>1,2,3</sup>, Qunli Zhang<sup>1,2,3</sup>, and Jianhua Yao<sup>1,2,3,\*</sup>

<sup>1</sup> College of Mechanical Engineering, Zhejiang University of Technology, Hangzhou, PR China

<sup>2</sup> Collaborative Innovation Center of High-end Laser Manufacturing Equipment (National “2011 Plan”), Zhejiang University of Technology, Hangzhou, PR China

<sup>3</sup> Institute of Laser Advanced Manufacturing, Zhejiang University of Technology, Hangzhou, PR China

Received: 9 December 2025 / Accepted: 3 May 2026

**Abstract.** Light, as a pivotal and versatile energy source, has given rise to a multitude of additive manufacturing (AM) technologies, collectively termed light-derived additive manufacturing (LDAM). This review provides a critical overview of recent advances in four principal categories: Laser Powder Bed Fusion (LPBF), Vat Photopolymerization (VPP), Laser Direct Writing (LDW), and Laser Metal Deposition (LMD). For each technology, we dissect the underlying principles, highlight groundbreaking studies and identify persistent challenges such as defect control in LPBF, material limitations in LMD, and speed-resolution trade-offs in VPP and LDW. The review further offers a unique comparative analysis through technology selection maps, guiding researchers in choosing the appropriate light-based AM process for their specific material and performance requirements. It aims to provide an overview of the current advances of research in this area, identify the still existing challenges and assess the trends and solutions related to specific studies. It expects that this review will prove invaluable reference to researchers and practitioners of AM technology, and that our efforts in this evolving area will contribute to the further advancement of AM.

**Keywords:** Light-derived additive manufacturing / laser powder bed fusion / vat photopolymerization / laser direct writing / laser metal deposition

## 1 Introduction

Differing from traditional subtractive manufacturing, additive manufacturing (AM), also known as 3D printing, by constructing objects layer by layer from the bottom up [1,2]. A key advantage of AM is the ability to directly realize customized design and fabrication with high speed and precision, especially those with complex geometries and internal structures that are unattainable through traditional manufacturing strategies [1,3]. Since its inception in the 1980s, AM has undergone substantial development and progress, especially over the past two decades, significantly impacting fields such as aerospace, education, medical, architectural, artistic, and automotive applications [2,4,5]. Furthermore, the maturity of AM applications varies in different fields, with its current applications in high value-added fields such as aerospace and medical being more advanced, and those in other fields still requiring further promotion [2,6].

With ongoing innovation and breakthroughs in fundamental principles, a diverse range of AM technologies have emerged and developed, such as Sheet Lamination (SHL), Layered Object Manufacturing (LOM), Materials Extrusion (MEX, Fused Deposition Modelling (FDM), Direct Ink Writing (DIW)), Binder jetting (BJT), Materials jetting (MJT, Ink Jet Printing (IJP)), Powder Bed Fusion (PBF, Laser Powder Bed Fusion (LPBF, (Selective Laser Melting (SLM), Selective Laser Sintering (SLS))), Vat photopolymerization (VPP, Stereo Lithography Appearance (SLA), Digital Light Processing (DLP), Two-photon polymerization (TPP)), Directed Energy Deposition (DED, Wire and Arc Additive Manufacturing (WAAM), Electron Beam Freeform Fabrication (EBF), Electron Beam Melting (EBM), Laser metal deposition (LMD)) etc. [2,7–13]. Although numerous AM technologies exist, the primary driving force include light, arc, electron beam, heat and pressure, among others; And the materials employed in these process are typically categorized as metallic, polymeric, inorganic and composite [1–3,7–12]. Utilizing these driving force, the aforementioned materials in powder, wire or paste form, are deposited layer by layer

\* Corresponding author: [lam@zjut.edu.cn](mailto:lam@zjut.edu.cn)

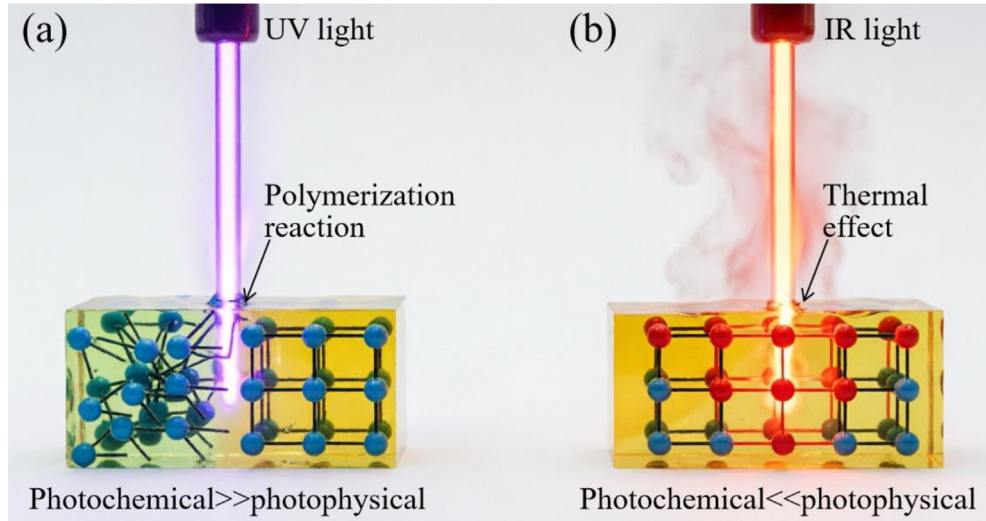


**Fig. 1.** Interaction of light and materials. (a) Photochemical > photophysical, breaking chemical bonds and polymerizing molecules, (b) photochemical < photophysical, exhibiting thermal effect.

at predetermined positions as specified. Each AM technology possesses a distinctive history, along with specific strengths and weaknesses, and encounters significant obstacles in practical applications [2]. Key challenges impeding the widespread adoption of AM include materials limitations (insufficient quantity and inadequate performance), process inefficiencies (slow manufacturing speed, low efficiency and lack of creative approach), and economic factors (high cost of fabrication) [2,8].

To advance the field of AM, it is essential to analyze the current state and address the challenges hindering its development. Given that light serves as a pivotal energy source in AM and plays a crucial role in numerous AM technologies, this review utilizes it as a point of entry to illustrate the current progress and future prospects of AM. In comparison to other energy sources, light or laser offer the advantages such as greater flexibility in manipulation and higher manufacturing accuracy, which facilitates the fabrication of high-precision complex structures; they also provide broad applicability due to compatibility with various additive manufacturing processes and materials, along with the ability to achieve environmentally friendly manufacturing with low energy consumption [14,15]. The primary limitations involve the limited penetration depth of light, which restricts the manufacturing depth; the potential for focused light to induce thermal stress and defects; and challenges in the fabricating large-scale components. For example, laser, a form of light, characterized as excited optical radiation, are highly directional, monochromatic, coherent and bright, and have numerous applications across various industries, particularly in materials processing [16,17]. As a type of electromagnetic radiation, light exhibits a spectrum of wavelengths from ultraviolet (UV) to infrared (IR), as well as intensities, and interacts with diverse materials, including solids, liquids and even gases. The interaction between light and materials involves two steps: photon absorption and energy transfer [18]. Materials absorb the photon energy through light-induced electron excitation, which

subsequently induces lattice phonon vibration, with phonon vibration predominantly manifesting as the thermal effect.

Based on the interactions of light and materials, the outcomes can be categorized into two processes (Fig. 1): if the light-induced excitation rate exceeds the thermalization rate, the excitation effect dominates, resulting in a photochemical process where light-electron interaction will break chemical bonds and polymerize the molecules; conversely, if the excitation rate is lower than the thermalization rate, it manifests as a photophysical process, also called photothermal process. The targeted application of the photochemical and photothermal effects has driven the development of numerous AM technologies. The photochemical processes are non-thermal material modification process, where the higher excitation energies break the chemical bonds and polymerize the molecules [19]. Considerable AM technologies leverage this effect, include DLP, SLA, TPP, and others. Photophysical effect involve the transformation of absorbed photo energy into heat [19]. AM technologies that utilize the thermal effects of lasers, includes SLM, SLS, and LMD, and so on. In the former process, UV light or lasers are commonly used to induce targeted effects; in the latter, IR lasers are typically employed to generate thermal effect.

We conducted a meticulous examination of the literatures on LDAM in the journals of *Science* and *Nature* in recent years, with LDAM being broadly classified into laser powder bed fusion (LPBF), vat photopolymerization (VPP), laser direct writing (LDW), and laser metal deposition (LMD) (Fig. 2). Given the pivotal role of light in AM, this review is structured to provide a detailed investigation of the major LDAM technologies. We begin with an in-depth analysis of LPBF and LMD for metals, focusing on advances in understanding melt pool dynamics and developing novel alloys. This is followed by a comprehensive review of VPP techniques, including SLA, DLP, TPP, and emerging volumetric AM (VAM)

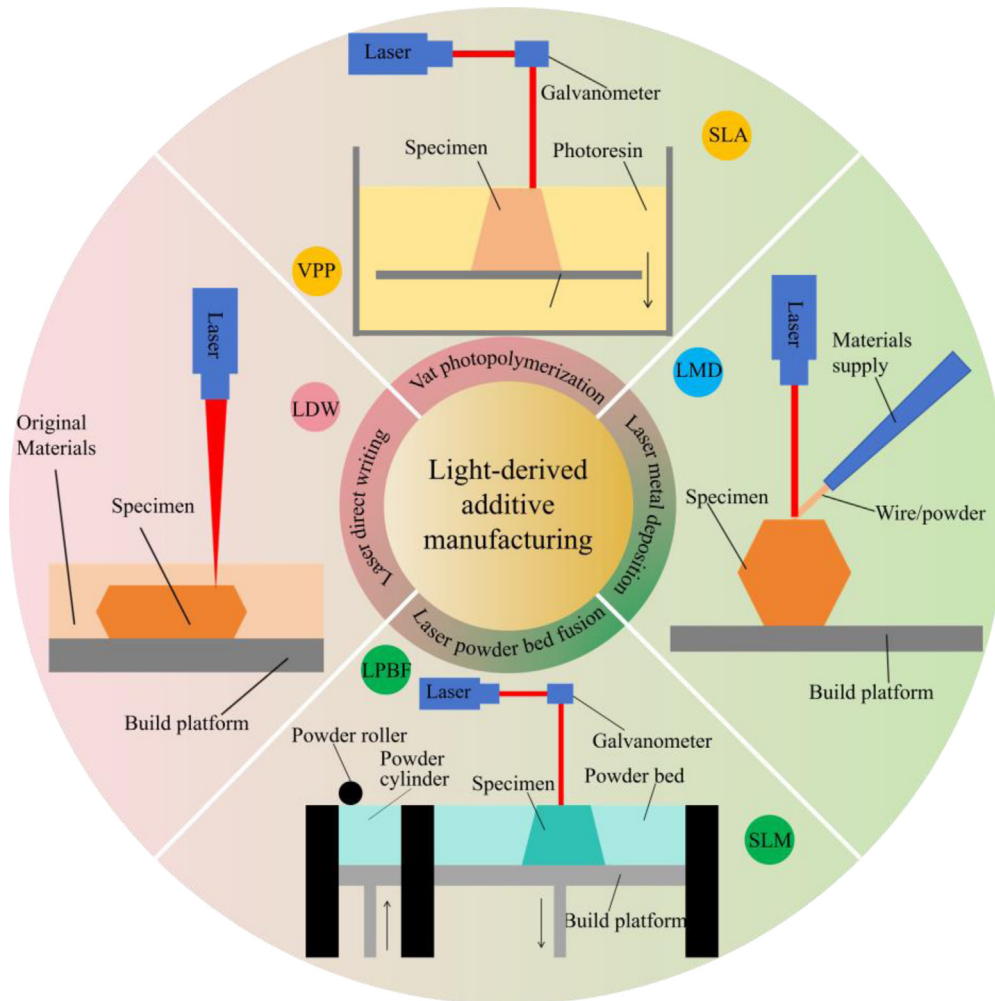


Fig. 2. LDAM and representative schematic diagram [2,8,20].

methods, highlighting their unparalleled precision and applications in functional materials. The discussion then proceeds to the high-resolution capabilities of LDW, follow by a dedicated section on technology selection that provides practical guidance. Finally, the review concludes with a critical assessment of the key challenges in the field, and on this basis, delineating prioritized and promising future research directions to advance both fundamental principles and practical applications.

## 2 Advances, challenges and countermeasures of LDAM

### 2.1 LPBF

LPBF is a mainstream technology in the field of laser additive manufacturing, enabling the production of complex parts with intricate geometries and precise features [8,21]. LPBF process encompasses commonly used printing techniques: selective laser melting (SLM, also direct metal laser sintering (DMLS)) and selective laser sintering (SLS) [22,23]. As shown in Figure 2, the main processes are followings [21–24]: (1) A layer of material is applied to cover the build platform. (2) A laser is employed

to fuse the initial layer or cross section of the model. (3) A new layer of powder is then spread across the previous layer using a roller. (4) Subsequently, additional layers or cross sections are fused and incorporated. (5) The process is repeated until the entire model is created. (6) The powder, which has not been fused, remains in position but is subsequently removed during the post-processing stage.

Nevertheless, several technical challenges must be overcome before LPBF can fully achieve its potential as a disruptive manufacturing technology [21,25–33]. Keyholes are deep vapor depressions that become unstable under certain laser parameters (high power, low speed), leading to trapped pores [25]. A primary challenge is controlling the interdependent dynamics among the laser, powder, and melt pool [21,26]. Additionally, achieving sufficient temporal resolution to detect the stochastic formation of keyhole pores presents a major hurdle [27,28]. Contemporary materials and methodologies frequently exhibit limitation in achieving balanced properties. High-strength alloys commonly exhibit limited ductility or inadequate fatigue resistance, primarily attributed to microstructural defects such as voids or phase heterogeneity [32,33]. To address practical demands, it is often necessary to employ innovative, model-driven alloy designs

**Table 1.** Representative recent studies on LPBF technology.

Technologies	Challenges	Materials and methods	References
SLM (laser)	Emergence and evolution of the defects remain unclear	SS316L; High-fidelity simulations, synchrotron experiments	[25]
		Ti-6Al-4V; High-speed X-ray imaging	[21]
		Ti-6Al-4V; Ultrahigh-speed synchrotron X-ray imaging	[26]
	Detection and imaging of the keyhole formation process remain a significant challenge	Ti-6Al-4V; High-speed synchrotron X-ray imaging, thermal imaging and multiphysics simulations; Machine learning	[27]
		AlSi10Mg; High-speed synchrotron X-ray imaging and a transverse magnetic field	[28]
		Ti-6Al-4V and 316L; In situ concentration modulations	[29]
		NiCoCr-based alloy with dispersing nanoscale Y <sub>2</sub> O <sub>3</sub> ; Model-driven alloy design approach	[30]
	Methods and materials used in AM technology remain insufficient	Ti-5Al-5Mo-5V-3Cr; Adding 5.0 wt% Mo	[31]
		High-entropy alloys AlCoCrFeNi <sub>2.1</sub> ; Controlling microstructure	[32]
		Ti-6Al-4V; Hot isostatic pressing and solution treatment and ageing	[33]
Comprehensive mechanical properties remain unsatisfactory			
SLS (laser)		Nylon plastic and aluminium; Discrete-element simulations, structure design	[34]

or specialized in-situ methods for creating heterogeneous microstructures [29–31]. Alternatively, extensive post-processing is required to eliminate defects and achieve optimal properties, thereby increasing both cost and complexity.

In a typical LPBF process, a high-power laser beam is employed to locally melt and solidify metal powders, thereby forming three-dimensional (3D) objects layer by layer [8,21]. The extreme thermal conditions during the printing process give rise to transient phenomena and complex structural dynamics. The interaction of these factors frequently results in the formation of structural defects, such as porosity. Some porosity is associated with deep, narrow, and unstable vapor depression zones, known as keyholes, which are caused by the excessive input of laser energy under high-power and low-scanning speed conditions [21,27]. Table 1 summarizes the detailed researches of LPBF technology.

Although LPBF has made significant progress, the emergence and evolution of the defects remain unclear. Therefore, Zhao et al. utilized high-speed X-ray imaging to in situ observe the detailed formation process of pores in Ti-6Al-4V, resulting from a critical instability at the keyhole tip [21]. This study revealed that the boundary of the keyhole porosity regime is sharp and smooth within the power-velocity space, with minimal variation between the bare plate and powder bed. Furthermore, the critical

keyhole instability generates acoustic waves within the melt pool, serving as an additional yet crucial driving mechanism for pores near the keyhole tip to migrate away from the keyhole and become trapped as defects. Further, Khairallah et al. employed high-fidelity simulations combined with synchrotron experiments to investigate the rapid multi-transient dynamics at the meso-nanosecond scale [25]. This work revealed novel spatter-induced defect formation mechanisms, which depend on the scan strategy and a competition between laser shadowing and expulsion. Subsequently, criteria for stabilizing melt pool dynamics and minimizing defects were established. Therefore, defects primarily form through two mechanisms: pores generated by keyhole tip instability and spatter-induced defects.

To date, the detecting and imaging of the keyhole formation process remain a significant challenge in which the crucial point is to control the complex laser-powder-melt pool interdependency dynamics. By integrating simultaneous high-speed synchrotron X-ray imaging with thermal imaging and multi-physics simulations, Ren et al. discovered two distinct types of keyhole oscillations in LPBF process of Ti-6Al-4V (Fig. 3) [27]. Operando X-ray imaging enables the acquisition of ground-truth data, allowing keyhole pore generation in LPBF samples to be detected with 100% accuracy and sub-millisecond temporal resolution. Moreover, the strategies of monitoring keyhole

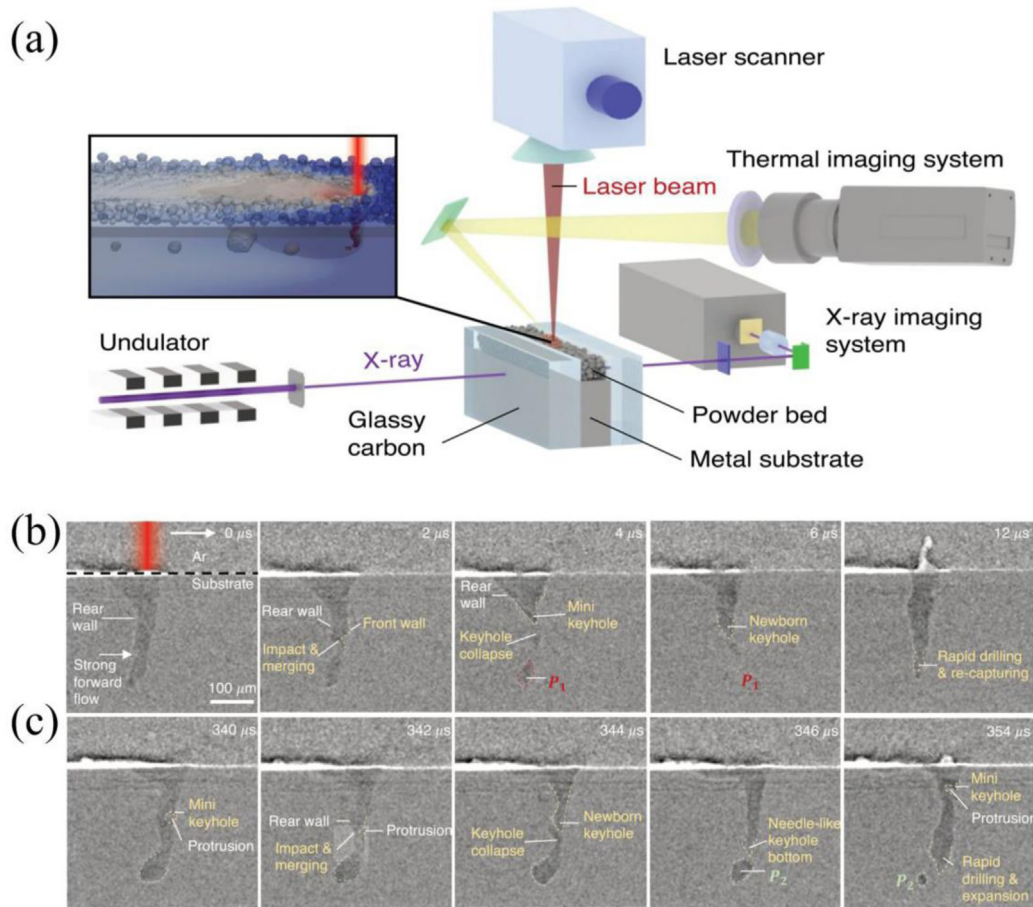


**Fig. 3.** Real-time keyhole detection in LPBF. (a) Schematic of the simultaneous synchrotron X-ray and thermal imaging experiment, (b) Megahertz X-ray images of intrinsic keyhole oscillation with no keyhole pore generated, (c) Megahertz X-ray images of perturbative keyhole oscillation with a keyhole pore generated. (reprinted with permission from Ref. [27]).

and melt pool oscillation behavior to identify anomalies prove both generic and practical. For example, Cunningham *et al.* employed ultrahigh-speed synchrotron X-ray imaging to quantify the vapor depressions (also keyholes) during laser melting of metals powder [26]. The direct visualization of the keyhole morphology and dynamics reveals that: (i) keyholes exist across the entire range of power and scanning velocity employed in LPBF; (ii) a well-defined threshold in laser power density marks the transition from conduction mode to keyhole mode; and (iii) the transition follows the sequences of vaporization, liquid surface depression, instability, and deep keyhole formation. Consequently, these findings have advanced a deeper understanding of the progress monitoring and formation mechanism of keyholes in the LPBF process.

The current methods and materials used in AM technology remain insufficient to meet more practical demands; therefore, the predominant approach addressing this challenge involves utilizing existing materials and adapting certain techniques to enhance comprehensive performance. For example, Zhang *et al.* developed an in situ LPBF method to spatially modulate alloy concentrations by partially homogenizing Ti-6Al-4V with a trace amount of 316L stainless steel [29]. This process achieved

micrometer-scale concentration gradients of 316L components within the Ti-6Al-4V matrix, resulting in the formation of a fine-scale  $\beta+\alpha$  dual-phase microstructure. This microstructure enhanced transformation-induced plasticity, thereby yielding high tensile strength (1.3 GPa), uniform elongation (9%), and exceptional work-hardening capacity (>300 MPa). This approach established a pathway for designing concentration-modulated heterogeneous alloys for structural and functional applications. In another study, an inorganic-reinforced metal material was developed, specifically a novel  $Y_2O_3$ -dispersion-strengthened NiCoCr alloy designed through modeling and laser additive manufacturing [30]. The microstructure analysis confirmed the successful incorporation of oxide dispersoids, which resulted in a two-fold improvement in strength and oxidation resistance, along with a 1,000-fold increase in creep resistance compared to conventional nickel-based alloys. These outcomes underscore the advantage of model-driven alloy design over traditional trial-and-error approaches in terms of efficiency. Through such in-process material modification, expectable microstructural features can be obtained, allowing desired mechanical properties to be achieved directly from the AM process.

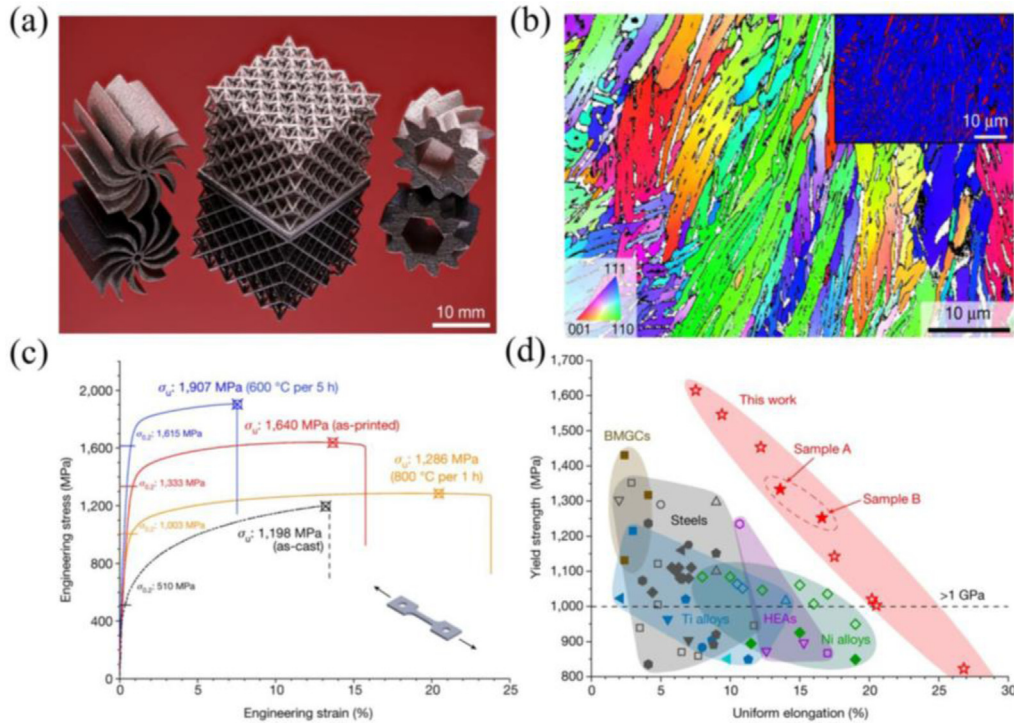


**Fig. 4.** AlCoCrFeNi<sub>2.1</sub> high-entropy alloys fabricated by LPBF process. (a) Manufactured heatsink with fan, octet lattice and gear, (b) A cross-sectional EBSD IPF map, (c) Tensile stress-strain curves, (d) Tensile yield strength versus uniform elongation compared with other high-performance AM metal alloys. (reprinted with permission from Ref. [32]).

Despite the extensive research on AM, the overall mechanical properties of components fabricated by this technology remain suboptimal, such as high-strength alloys often exhibiting limited ductility and fatigue properties. To address this challenge, Ren *et al.* utilized the LPBF technology to produce AlCoCrFeNi<sub>2.1</sub> high-entropy alloys (HEAs) featuring dual-phase nanolamellae (Fig. 4) [32]. The resulting material exhibited a remarkable yield strength of 1.3 GPa and an elongation of 14%, surpassing the properties of other metal alloys manufactured by AM. The high strength is attributed to the alternating face-centered cubic (FCC) and body-centered cubic (BCC) nanolamellae, with the BCC phase contributing enhanced strength and work hardening capability. Conversely, ductility originates from the hierarchical microstructure of the dual-phase nanolamellae within eutectic colonies, which promotes isotropic mechanical behavior. Nevertheless, the potential of AM for structural applications is frequently constrained by inadequate fatigue properties, primarily attributable to microvoids formed during the fabrication process. To address this issue, Qu *et al.* developed a Net-AM processing technique to prepare approximate void-free Ti-6Al-4V components through optimizing behaviors of phase transformation and grain growth [33]. Their study evaluated the fatigue resistance of these titanium alloy components and revealed a high fatigue limit of approximately 1 GPa, surpassing those of all AM-processed and forged titanium alloys, as well as other metallic materials. Consequently, the adoption of innovative methods and understanding of

strengthening mechanism facilitate the design of alloys with high strength and fatigue performance in the AM process, supporting their broader engineering applications.

## 2.2 LMD

Directed energy deposition (DED) is a branch of AM technologies in which a feedstock material, typically in powder or wire, is delivered to a substrate. Simultaneously, an energy source, such as a laser beam, electron beam, or plasma/electric arc, is focused on the substrate, thus forming a small melt pool and the continuous material deposition in a layer-by-layer style [35]. Based on the energy source and type of feedstock, commercially available technologies are designated as laser metal deposition (LMD), directed metal deposition (DMD), laser solid forming (LSF), directed light fabrication (DLF), electron beam additive manufacturing (EBAM), and wire arc additive manufacturing (WAAM) [35,36]. LMD processes offer a number of distinctive advantages over other AM techniques [36]. Specifically, LMD techniques are capable of producing near-net shapes, such as large components that exceed the build volume of LPBF processes. Furthermore, LMD techniques are highly efficient for the repair of damaged or worn-out components, and for adding new features to existing components. Other advantages include the ability to fabricate functionally graded materials, higher deposition rates, and a more comprehensive processing window for the optimizing finished components. As shown in Figure 2, the LMD

**Table 2.** Representative studies of LMD technology.

Technologies	Challenges	Materials and methods	References
LMD (laser)	Limited availability of new materials	NiTi; Localized molten environment and near-eutectic mixing of elemental powders	[38]
		Ti-O-Fe; Atom probe tomography	[39]
		Fe19Ni5Ti; Cyclic re-heating	[40]
		Ti-Cu alloy; Controlling elements and microstructures	[41]

processes are followings [36,37]: (1) A laser beam and powder metals are fed through the nozzle and deposited onto a metallic substrate. (2) The powder is melted by the laser heat, resulting in the formation of a metal pool on the solid substrate through fusion bonding. (3) The laser head and powder delivery nozzle are commenced to ascent. (4) The entire process is conducted until the final near-net shape of the metal component is achieved. Table 2 showed the detailed researches on LMD technology.

While LMDs offer numerous advantages, they also present a number of challenges in both research and practical application, such as the scarcity of novel materials suitable for this technique. It is generally acknowledged that oxygen (O) and iron (Fe) are inherent impurity elements in sponge titanium. On the contrary, Song *et al.* employed these elements serving as the  $\alpha$ - and  $\beta$ -stabilizing elements of Ti, respectively, to prepare titanium-oxygen-iron alloys by precise elemental modulation [39]. In the study, alloy design were integrated with LMD process to develop a series of titanium-oxygen-iron compositions that exhibit exceptional tensile properties (Fig. 5). Four levels of O (0.15%, 0.35%, 0.50%, 0.70%) were thus considered with 3% Fe and balanced Ti, leading to ten experimental alloys. The atomic-scale origins of these properties are elucidated through the application of diverse characterization techniques. The abundance of oxygen and iron, combined with the simplicity of net-shape or near-net-shape fabrication by AM, render these  $\alpha$ - $\beta$  titanium-oxygen-iron alloys attractive for a diverse array of applications. In another study, Kürnsteiner *et al.* had developed a new material (Fe19Ni5Ti) comprising alternating soft and hard layers by LMD, which drew inspiration from the unique composition of ancient Damascus steels [40]. This material exhibited tensile strength of 1,300 MPa and an elongation of 10%, demonstrating superior mechanical properties compared to those of ancient Damascus steel. The principles of in situ precipitation strengthening and local microstructure control can be applied for a wide range of precipitation-hardened alloys and different AM processes. Therefore, the design of new materials is an effective approach to addressing challenges and enhancing material performance.

The development of new materials is highly challenging, while a comprehensive investigation of existing materials and techniques can yield unexpected outcomes. For instance, Zhang *et al.* reported titanium-copper alloys that exhibited high constitutional supercooling resulting from the partitioning of alloying elements during solidification [41]. This approach mitigated the issues associated

with high thermal gradients in laser-melted AM. The as-printed specimens displayed a fully equiaxed fine-grained microstructure, exhibiting enhanced mechanical properties, including high yield strength and uniform elongation. These properties were attributed to the formation of an ultrafine eutectoid microstructure, achieved by utilizing high cooling rates and thermal cycles without the necessity for special process control or additional treatment. In addition, microstructure modulation is another effective approach to improve the mechanical properties of materials. For example, Hou *et al.* developed a thermodynamically efficient, low-hysteresis elastocaloric cooling NiTi material by employing a localized molten environment, near-eutectic mixing of elemental powders and LMD process [38]. This approach resulted in the formation of nanocomposite microstructures, comprising a Ni-rich intermetallic compound interspersed within a binary alloy matrix (Fig. 6). The incorporation of nanocomposite microstructures had been demonstrated to enhance material efficiency by a factor of four to seven, thereby ensuring ultra-low hysteresis and repeatable performance over one million cycles. AM technology allows for precise control of high-performance metallic refrigerants, extending operational lifespan. Therefore, a comprehensive investigation of existing materials integrated with AM techniques to manipulate microstructures, can significantly enhance properties, such as high strength, high toughness, and long service life.

### 2.3 Vat photopolymerization

Vat photopolymerization (VPP), one of the earliest and most pervasive AM technologies, exerts a profound influence on numerous industries [42]. As is shown in Figure 2, the VPP involves exposing photo-sensitive materials to controlled doses of light to form polymerized material layers, with these layers subsequently combined to construct a 3D object [43,44]. Compared to other AM technologies, it exhibits a number of outstanding advantages, including high precision, high speed, low cost, the production of aesthetically pleasing parts, and a versatility across a wide range of applications [42]. Basing on the variation of curing source, VPP can further be classified into SLA, DLP, Continuous Liquid Interface Production (CLIP), TPP and VAM, among others [45,46].

SLA utilizes a UV or purple laser beam to perform point-wise scanning across the surface of a liquid photopolymer resin, curing the material layer by layer [47–49]. It enables the fabrication of parts with high

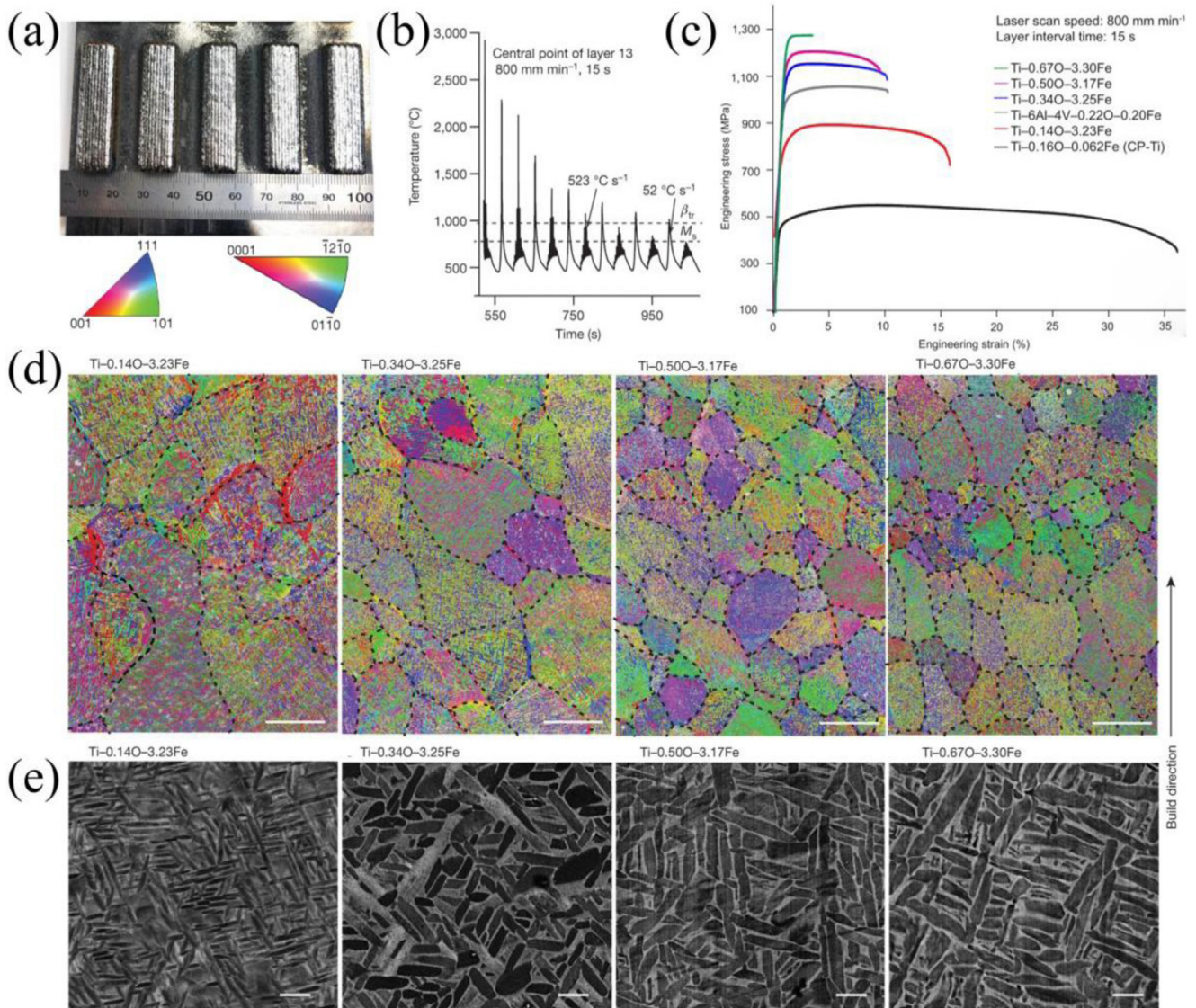


**Fig. 5.** Ti-O-Fe alloy fabricated by LMD. (a) As-built rectangular Ti-0.34O-3.25Fe coupons, (b) Temperature profile of the central point of layer 13 in a 25-layer coupon by simulation, (c) Tensile properties of LMD-printed Ti-O-Fe alloys, (d) Electron backscatter diffraction (EBSD) inverse pole figure images, (e) Backscattered electron images. (reprinted with permission from Ref. [39]).

dimensional accuracy, albeit with comparatively limited build speed. DLP employs a digital projector to flash a full-layer image onto the resin vat, curing an entire cross-section simultaneously [50–54]. Compared to SLA, it features faster printing speed, but with a corresponding decrease in resolution. TPP leverages the nonlinear two-photon absorption effect, induced by an ultrafast femto-second laser, to initiate polymerization exclusively within a sub-diffraction-limited volume at the focal point of laser [55–60]. This grants the technique nanometer-scale resolution, with trade-offs including very slow build rates and exceptionally high costs. CLIP, an advanced variant of DLP, enables continuous printing via an oxygen-inhibited dead zone [61,62]. It eliminates layer separation, significantly increases print speed, and produces smooth surfaces, but imposes stringent demands on resin chemistry and

process control. VAM uses intersecting light beams to solidify rotating resin nearly instantly, enabling support-free, smooth prints in seconds, though material choices are limited and achieving uniform high resolution remains challenging [63–68].

Using SLA as example, the mainly processes (Fig. 2) are followings [43,45]: (1) The build platform is lowered from the top of the resin vat by a distance equal to the layer thickness. (2) An UV light is employed to cure the resin layer in a successive manner. (3) The platform continues its descent, with each subsequent layer being constructed atop the previous one. (4) A blade is employed to scrape the surface of resin to create a uniform resin layer on the specimen for the next curing process. (5) Upon completion, the resin is drained from the vat, and the object is removed. Table 3 showed the detailed researches of VPP technology.

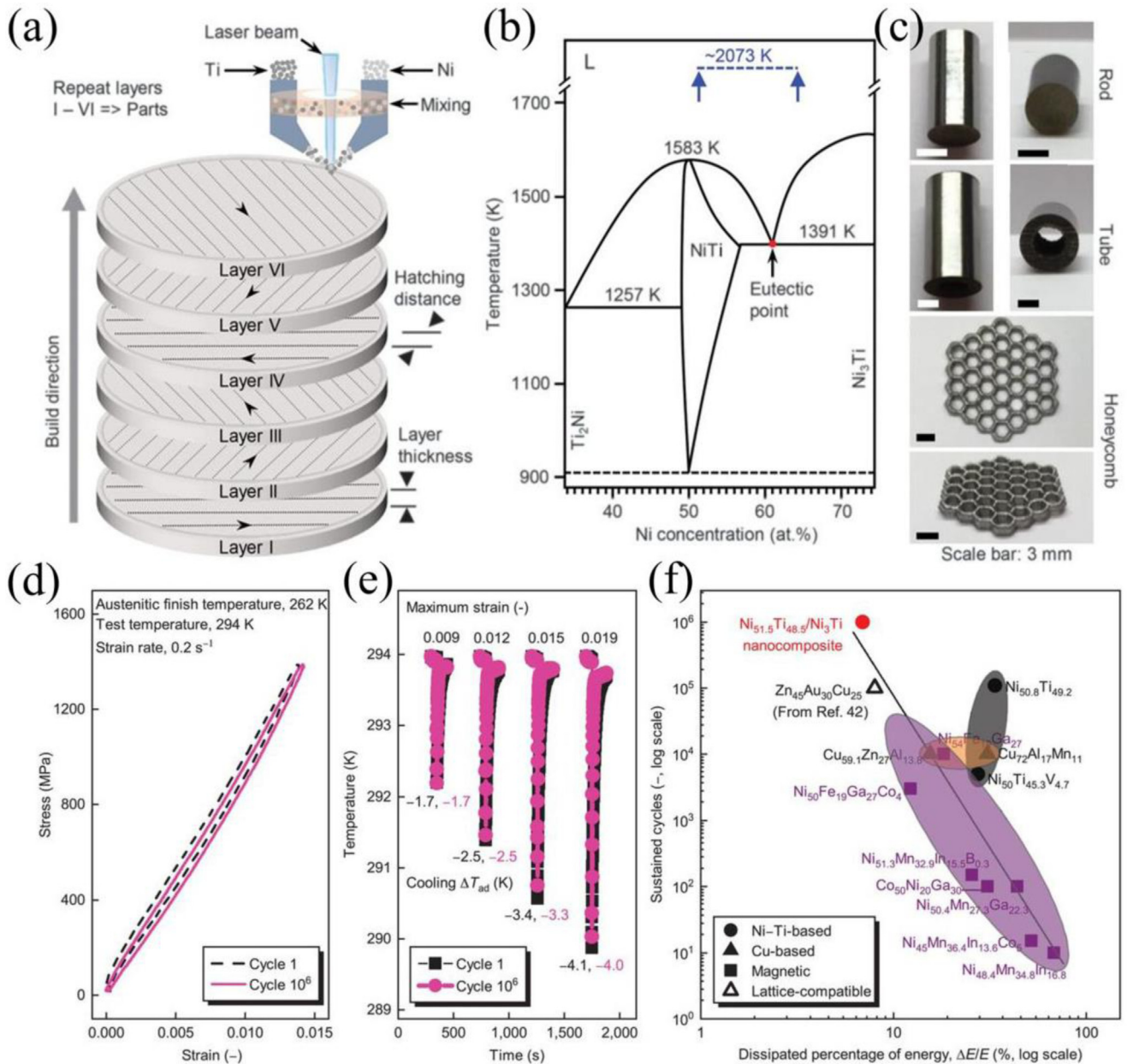


**Fig. 6.** Elastocaloric NiTi nanocomposite manufactured by LMD. (a) Schematic representation of an LMD process, (b) Phase diagram of NiTi, (c) Photographs of LMD-produced NiTi nanocomposite rods, tubes, and honeycombs, (d) Compressive stress-strain curves, (e) Elastocaloric cooling, (f) Log-log plot of the dissipated fraction of input energy versus sustained compressive cycles. (reprinted with permission from Ref. [38]).

### 2.3.1 SLA

SLA is the first commercially available 3D printing technique, developed by Chuck Hull in 1986. An SLA equipment comprises a container for photocurable liquid resin, a laser source (typically UV light) to stimulate polymerization and crosslinking of the liquid resin, a system enabling the horizontal (X-Y) movement of the laser beam and controlling the vertical (Z-direction) movement of the fabrication platform [71].

The development of artificial tissues or organs utilizing biocompatible gel materials, stem cells, and AM technology represents a complex challenge. A key difficulty in this

process is the generation of blood vessels within these constructs, which are crucial for transporting nutrients to the cells. The SLA technique, with high resolution and precision, was employed to generate the intricate network of intertwined blood vessels in artificial organs [47]. This technique is capable of manufacturing tubes for the transportation of air, lymphatic fluids, and other substances. In the experiments, a novel AM technique was employed to cut the 3D design into 2D slices, which are then printed layer by layer under the control of software, with each layer cured using a blue light. The team fabricated a hydrogel model that mimicked an alveolus with preliminary functionality, representing airways

**Table 3.** Representative studies of VPP technology.

Technologies	Challenges	Materials and methods	References
SLA (laser)	Generation of blood vessels remains challenging	Photopolymerizable hydrogels; Using food dye additives as biocompatible photoabsorbers	[47]
	Photosensitive resin remains not recyclable	Photopolymer resin; New resin derived from renewable lipoates	[48]
DLP (UV light)	Performance and diversity of printable materials are limited	Photopolymer resin; Dissociation of the dithioacetal bonds	[49]
		Zirconate titanate (PZT); 3D lattice with piezoelectric effect	[50]
		(18C6@K)2ZrCl4Br2; Multimaterial digital light-printing method	[51]
		Metal precursors(Cu, Ni, CuNi, CuNiCoFe, W-Ni); Precursor method	[52]
TPP (laser)	Low manufacturing speed and efficiency; Limited applications	Resin precursor; Precursor method	[53]
		Photoresin; Adjusting the light dose	[54]
		Polyhedral oligomeric silsesquioxane (POSS)resin; Precursor method	[55]
		CdSe/ZnS, PbS, TiO <sub>2</sub> and In <sub>2</sub> O <sub>3</sub> ; Laser direct printing of inorganic nanomaterials by using colloidal nanocrystals	[56]
		Photopolymer resist; Femtosecond (fs) laser proceeding	[57]
		Photoresin; Metalens-generated focal spot array	[58]
		Acrylate-based photoresist; Femtosecond laser photocuring	[59]
VAM (UV light and laser)	Limitations in speed, geometry, and surface quality	Acrylic polymer; TPP with postprinting oxygen plasma etching	[60]
		Photosensitive resin; VAM	[63]
		Photosensitive resin; Two-photon-based 3Dprinting.	[64]
		Photopolymer-silica nanocomposite; Microscale computed axial lithography and tomographically illuminating	[65]
		Photoswitchable photoinitiators; Xolography	[66]
		Bioink; Adaptive and context-aware VAM	[67]
		Photoresin; Digital incoherent synthesis of holographic light fields (DISH)	[68]
		Photopolymerizable resin; Combination single-digit, micron-resolution optics with continuous roll of film	[61]
CLIP (UV light)	Low efficiency of particle fabrication		
Laser pattern(laser)	Low speed and precision of nanofabrication	Hydrogel with photosensitive species; Femtosecond laser proceeding	[69]
Inject+laser?UV light?		Photosensitive resins; Vision-controlled jetting	[70]

capable of transporting oxygen to surrounding blood vessels. Therefore, the adoption of SLA technology addresses the demands for fabrication of complex structures in the biomedical field.

Currently, it is not feasible to depolymerize and reuse existing photopolymer resins in a circular and closed-loop pathway. To address this challenge, Machado *et al.* presented a compelling argument for the potential of photopolymer resins to be depolymerized and reused in a circular manner [48]. Their study described a photopolymer resin derived entirely from renewable lipoates that can be 3D-printed into high-resolution parts, efficiently deconstructed, and subsequently reprinted in a circular manner. The limitations of previous methods that employed internal dynamic covalent bonds for recycling and reprinting 3D-printed photopolymers have been addressed by replacing conventional (meth)acrylates with dynamic cyclic disulfide units derived from lipoates. The lipoate-based resin is highly modular, allowing for the composition and network architecture to be adjusted to create printed materials with thermal and mechanical properties comparable to those of several commercial acrylic resins.

### 2.3.2 DLP

A digital micro mirror device is employed in DLP to project the 2D image of the corresponding slice file on the build plate and simultaneously cure the resin, thereby achieving a higher printing speed than that of SLA [72]. DLP printers employ a digital light projector to expose numerous layers of resin simultaneously, thereby ensuring homogeneous irradiance across the entire build area. Subsequent to the curing of a given layer, the build plate undergoes a slight upward movement, thereby dislodging the model from the transparent contacting window [45]. Subsequently, the build plate is relocated to the designated position, and the remaining resin is filled by capillary action. This process will be repeated until the final 3D structure is obtained. DLP printing can be classified into two distinct approaches, namely top-down and bottom-up, based on the movement of the build plate [73]. While DLP has advanced considerably, significant challenges persist in its further development. For example, in DLP process, the adhesive forces between the interface and the printed object could hinder the printing speed. To address challenge, Walker *et al.* introduced a novel approach for the fabrication of polymeric components that employed a mobile liquid interface (a fluorinated oil) to facilitate a continuous and rapid printing process, independent of the polymeric precursor [53]. The bed area was not constrained by thermal limitations due to the direct cooling effect of the flowing oil across the entire print area. The demonstration of continuous vertical print rates exceeding 430 mm/h with a volumetric throughput of 100 L/h, along with the production of proof-of-concept structures from hard plastics, ceramic precursors, and elastomers, substantiated the viability of this approach.

The emergence of DLP technology has enabled the fabrication of components that are challenging to produce by traditional means. While AM techniques allow for the

preparation of stimulus-responsive materials with 3D structures, but few structural materials have the same system complexity as biological. Hence, Cui *et al.* reported a design and manufacturing route to create a class of robotic metamaterials capable of exhibiting multiple degrees of freedom in their motion, amplifying strain in a prescribed direction in response to an electric field (and vice versa), and thus enabling programmed motions with integrated self-sensing and feedback control [50]. These robotic metamaterials were composed of networks of piezoelectric, conductive, and structural elements interwoven into a designed 3D lattice. The resulting architected materials function as proprioceptive microrobots, capable of active sensing and movement in response to their environment stimuli. Although AM offered significant advantages in preparing functional materials, it has yet to achieve substantial progress in luminescent materials. Based on this, Zhu *et al.* demonstrate a near-unity photoluminescence quantum yield (PLQY) with blue and green emission resulting from the supramolecular assembly of hafnium (Hf) and zirconium (Zr) halide octahedral clusters (Fig. 7) [51]. The (18C6@K)2HfBr6 powder exhibited blue emission with a PLQY of 96.2%, while the (18C6@K)2ZrCl4Br2 powder demonstrated green emission with a PLQY of 82.7%. These highly emissive powders were employed in thin-film displays and emissive 3D printed architectures, both exhibiting high spatial resolution. Consequently, DLP technology exhibit great potential for applications in the preparation of complex structured and functional materials.

### 2.3.3 TPP

The laser utilized in TPP has a longer wavelength, frequently near-infrared, and is distinctive in that it enables a phenomenon known as "two-photon absorption" [43]. In this process, two low-energy photons merge within a confined space, generating the energy necessary to initiate the polymerization process [45]. TPP with high precision enables the fabrication of intricate and delicate structures, making it an excellent choice for micro-optics and sensing applications. The resolution of this AM technique is approximately 150 nm, with a high resolution of up to 10 nm achieved by employing the stimulated emission depletion method under threshold conditions [45,46]. However, the serial point-by-point writing scheme of TPP is inadequate for many applications owing to its slow processing speed. Attempts at parallelization have either not achieved submicrometer resolution or have been unable to pattern complex structures. To address this issue, Saha *et al.* implemented a projection-based layer-by-layer parallelization by spatially and temporally focusing an ultrafast laser [57]. This approach increases the throughput by up to three orders of magnitude and expands the geometric design space.

Currently, AM of silica glass is dominated by technique that rely on traditional particle sintering, which limits the adoption of these techniques in microsystem technology and prevents technological breakthroughs. To address this issue, Bauer *et al.* developed a sinterless, two-photon polymerization AM approach for producing free-form fused

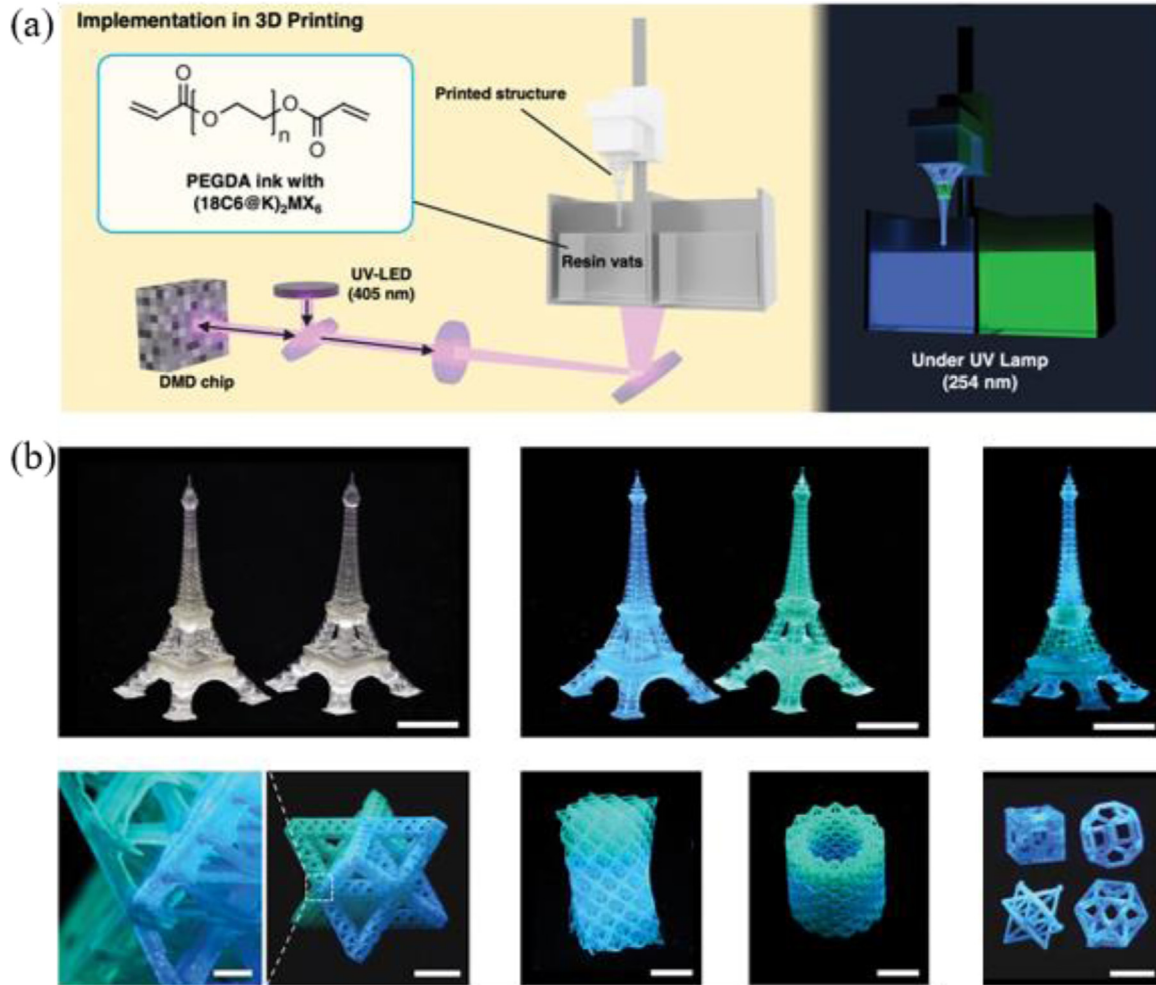


**Fig. 7.** Implementation of the blue-green dual-color AM. (a) Schematic illustrating the multimaterial AM process, (b) 3D-printed samples with varying hierarchical structures and geometric shapes. (reprinted with permission Ref. [51]).

silica nanostructures from a polyhedral oligomeric silsesquioxane (POSS) resin [55]. The POSS resin formed transparent fused silica at a markedly reduced temperature of only 650 °C, which was 500 °C lower than the typical sintering temperatures used to fuse discrete silica particles into glass. Concurrently, a fourfold enhancement in resolution was achieved, thereby enabling the development of visible light nanophotonics. Current AM technologies for inorganic materials typically utilize photocurable resins, which have been observed to reduce the purity of the materials and degrade the properties of the printed objects. To address this challenge, Li *et al.* proposed a general strategy for laser direct printing of inorganic nanomaterials by employing colloidal nanocrystals as the fundamental structural units and photochemically bonding them through their inherent ligands [56]. In the absence of resins, this bonding process generated arbitrary 3D structures characterized by a high inorganic mass fraction (~90%) and considerable mechanical strength. Therefore, TPP technology enables the sinterless or resin-free fabrication of inorganic nanostructures with high purity, precision and strength.

### 2.3.4 VAM

Despite the significant progress, the high-speed fabrication of soft objects with intricate geometries without layering artefacts remains a substantial challenge. Recent innovations have addressed this issue by incorporating chemical and optical nonlinearity into the photopolymerization, which, when combined with sophisticated hardware, enables VAM [74]. VAM, a relatively novel technique initially documented in 2017, partially addresses the limitations of conventional AM processes. Specifically, VAM circumvents the issues such as inferior surface quality and mechanical properties with the directional discrepancies, as parts are fabricated in a single step. This is achieved by selectively delivering energy to assigned points within a three-dimensional space in a medium, thereby initiating one or more reactions that generate a physical part [75]. VAM offers a number of advantages, including the elimination of the necessity for support structures and the ability to print highly viscous fluids or even solids. Additionally, it enables direct volumetric fabrication, which is significantly faster than traditional layer-by-layer

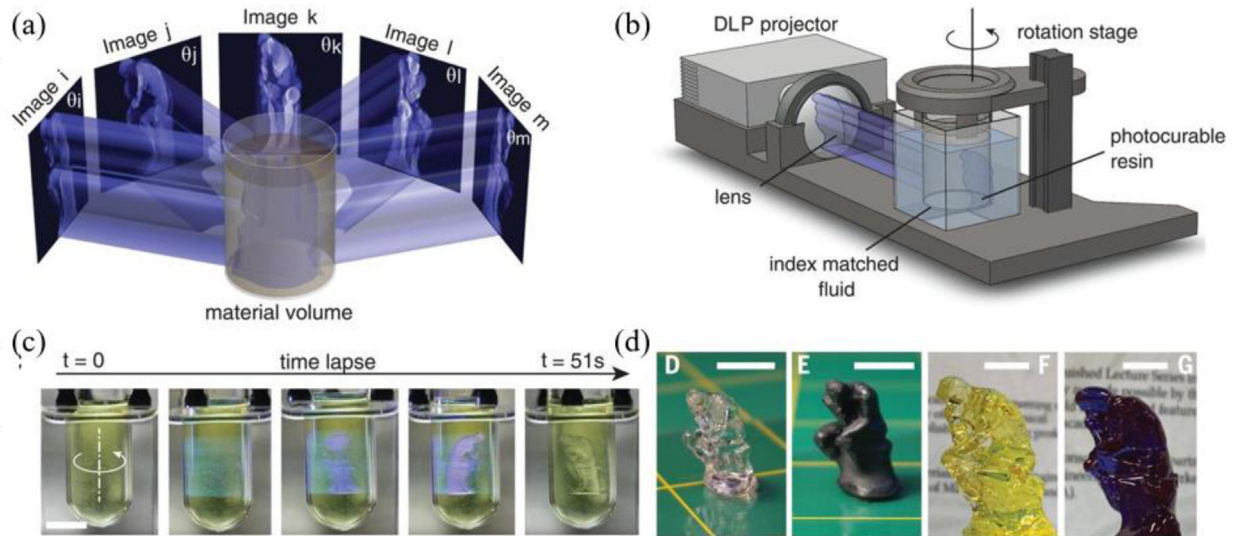


**Fig. 8.** CAL volumetric fabrication. (a) Underlying concept: Patterned illumination from many directions delivers a computed 3D exposure dose to a photoresponsive material, (b) Schematic of the CAL system used in this work. DLP projector, digital light processor-based projector. (c) Sequential view of the build volume during a CAL printing, (d) 3D-printed samples. (reprinted with permission Ref. [63]).

curing methods, allowing for orders-of-magnitude increase in print speeds and volumes. To date, numerous approaches for VAM have been developed, employing single- or multi-photon polymerization and leveraging optical and/or chemical nonlinearity to fabricate 3D objects [74,75]. The most prominent techniques in the field of VAM are computed axial lithography or tomographic VAM, two-photon polymerization (TPP), and light sheet printing techniques such as xolography.

Many research groups have employed effect of two-photon absorption for proceeding volumetric printing, while the laser power required for this process has restricted the print size and speed, impeding its widespread application in macrostructures. To address this challenge, Sanders *et al.* employed triplet fusion upconversion to achieve volumetric printing with less than 4 milliwatts of continuous-wave excitation. The upconversion process was incorporated into the resin through the use of encapsulation with a silica shell and solubilizing ligands [64]. Furthermore, an excitonic strategy was introduced to enable the systematic control of the upconversion threshold, thereby supporting either monovoxel or parallelized printing schemes. This approach allowed for printing at power densities that were several orders of magnitude lower than the power densities typically required for two-photon-based AM. In addition, Regehly *et al.* introduce xolography, a dual-color technique that employed photo-switchable photoinitiators to induce local polymerization within a confined monomer volume via linear excitation by intersecting light beams of different wavelengths [66]. This concept was demonstrated with a volumetric printer designed to generate 3D objects with complex structural features as well as mechanical and optical functions. Compared to the state-of-the-art VAM techniques, this method exhibits a resolution approximately ten times higher than computed axial lithography without feedback optimization, and a volume generation rate that is four to

five orders of magnitude higher than two-photon photopolymerization. It is anticipated that this technology will facilitate a significant transformation in the field of rapid volumetric production, enabling the fabrication of objects across a wide range of length scales, from nanoscopic to macroscopic scale. Therefore, by employing specialized photochemical processes to overcome traditional limitations, the efficiency and effectiveness of additive manufacturing have been enhanced.

The limitations in speed, geometry, and surface quality of AM processes are attributable to their dependence on material layers that significantly influences the performance of the final workpiece. Therefore, the complete elimination of this material layering would have a revolutionary impact on the field of AM technology. In a recent study, Kelly *et al.* developed a novel technique of computed axial lithograph for simultaneously printing all points within a 3D object, which involved exposing a rotating volume of photosensitive material to a dynamically evolving light pattern (Fig. 8) [63]. Their process successfully fabricated intricate details as fine as 0.3 millimeters in robust engineering acrylate polymers, as well as smooth-surfaced soft structures from gelatin methacrylate hydrogel. Notably, their process allows for the creation of components that can encapsulate existing solid objects, facilitating the fabrication of multimaterial designs. Consequently, manufacturing technology utilizing computed axial lithograph method to produce the whole component without non-layers structures in a single step, enhancing speed, geometric accuracy, and surface quality.

### 2.3.5 CLIP

Particle fabrication has recently garnered significant attention due to its diverse applications in bioengineering, drug and vaccine delivery, microfluidics, granular systems, self-assembly, microelectronics, and abrasives. In a recent

**Table 4.** Representative studies of LDW technology.

Technologies	Challenges	Materials and methods	References
Laser direct writing (laser)	Balance of high purity and excellent properties	CdSe/ZnS core/shell QDs; Photoexcitation-induced chemical bonding	[78]
		Perovskite nanocrystals; Ultrafast laser-induced liquid nanophase separation	[79]
		LiNbO <sub>3</sub> ; Laser-induced electric field	[80]

study, Kronenfeld *et al.* introduced a scalable, high-resolution, 3D printing technique for the fabrication of shape-specific particles based on roll-to-roll continuous liquid interface production (r2rCLIP) [61]. This technique employed single-digit, micron-resolution optics combined with a continuous roll of film, which enabled the rapid and versatile fabrication and harvesting of shape-specific particles from a variety of materials with complex geometries, including geometries that were not achievable with advanced mold-based techniques. The study demonstrates r2rCLIP production of both moldable and non-moldable shapes, achieving voxel sizes as small as  $2.0 \times 2.0 \mu\text{m}^2$  in the printing plane and an unsupported thickness of  $1.1 \pm 0.3 \mu\text{m}$ , with production speeds of up to 1,000,000 particles per day. Consequently, these microscopic particles with complex structures fabricated by novel r2rCLIP technique, capable of integration with intricate designs, hold potential for various applications in biomedical, analytical, and advanced materials fields.

### Laser direct writing

Laser direct writing (LDW) based on multi-photon polymerization (MPP) is an AM technology that enables the construction of readily assembled structures with a resolution of less than 100 nm [76,77]. As depicted in Figure 2, an ultra-fast laser beam is tightly focused into the volume of a transparent material, prompting the nonlinear absorption of two or more photons and undergo local polymerization. By scanning the beam along a path that corresponds to the design parameters of a 3D model, it is possible to fabricate an accurate micromodel that precisely reflects the original design [76]. LDW is a maskless, highly efficient, and cost-effective too for micro-/nanofabrication, extensively used in a various fields, such as micro-electromechanical systems (MEMS), photomasks, and various micro-/nanostructures [77]. Driven by the rapid advancement of nanotechnologies, the LDW system, with its enhanced fabrication resolution and broader application potential, has garnered considerable interest. Table 4 showed the detailed researches of LDW technology.

3D laser nanoprinting allows for the fabrication of a wide range of nanostructures with high precision and resolution, while the manufacturing of inorganic nanostructures typically necessitates the use of nanomaterial-polymer composites. This process is constrained by a photopolymerization mechanism, which results in a reduction of material purity and intrinsic properties. Given this, Liu *et al.* presented a new approach to developed a polymerization-independent LDW technique,

designated as photoexcitation-induced chemical bonding (Fig. 9) [78]. In the absence of additives, the holes generated within semiconductor quantum dots were transferred to the nanocrystal surface, thereby enhancing their chemical reactivity and facilitating interparticle chemical bonding. To demonstrate the potential of this approach, arbitrary 3D quantum dot architectures were successfully printed with a resolution that surpassed the diffraction limit. This strategy offered a promising route for the fabrication of free-form quantum dot optoelectronic devices, such as light-emitting devices and photodetectors.

The material composition, engineering, and device fabrication of perovskite nanocrystals (PNCs) in solution may introduce contamination from organic substances, necessitating multiple synthetic, processing, and stabilization steps. Additionally, PNCs, susceptible to degradation due to their inherent instability, may undergone the disruption of structural integrity, leading to a loss of optoelectronic performance when they exposed to light, heat, oxygen, water vapor, and other environmental factors. Therefore, Sun *et al.* developed a method for fabricating PNCs with tunable composition and bandgap in glass by LDW technology (Fig. 10) [79]. The PNCs demonstrated high stability against UV radiation, organic solvents, and elevated temperatures up to 250 °C. 3D structures in glass fabricated by LDW possess significant potentials for a variety of applications, including optical storage, micro-light emitting diodes, and holographic displays. In addition, Lithium niobate (LiNbO<sub>3</sub>) is regarded as a promising material for optical communications and quantum photonic chips, while the conventional electrical poling methods for ferroelectric domain engineering in optical, acoustic and electronic applications are limited to 2D space and micrometer-scale resolution. Consequently, Xu *et al.* developed a non-reciprocal near-infrared LDW technique for the reconfiguration of 3D ferroelectric domain structures in LiNbO<sub>3</sub> with nanoscale resolution [80]. The proposed method utilized a laser-induced electric field capable of writing or erasing domain structures in the crystal, depending on the laser writing direction. This approach enabled controllable nanoscale domain engineering in LiNbO<sub>3</sub> and other transparent ferroelectric crystals, which had the potential to be applied in high-efficiency frequency mixing, high-frequency acoustic resonators, and high-capacity non-volatile ferroelectric memory. Therefore, utilizing LDW technology to construct 3D structures and integrate functional properties within materials effectively prevents contamination, enhances purity, while significantly improving performance and expanding the scope of application environments.

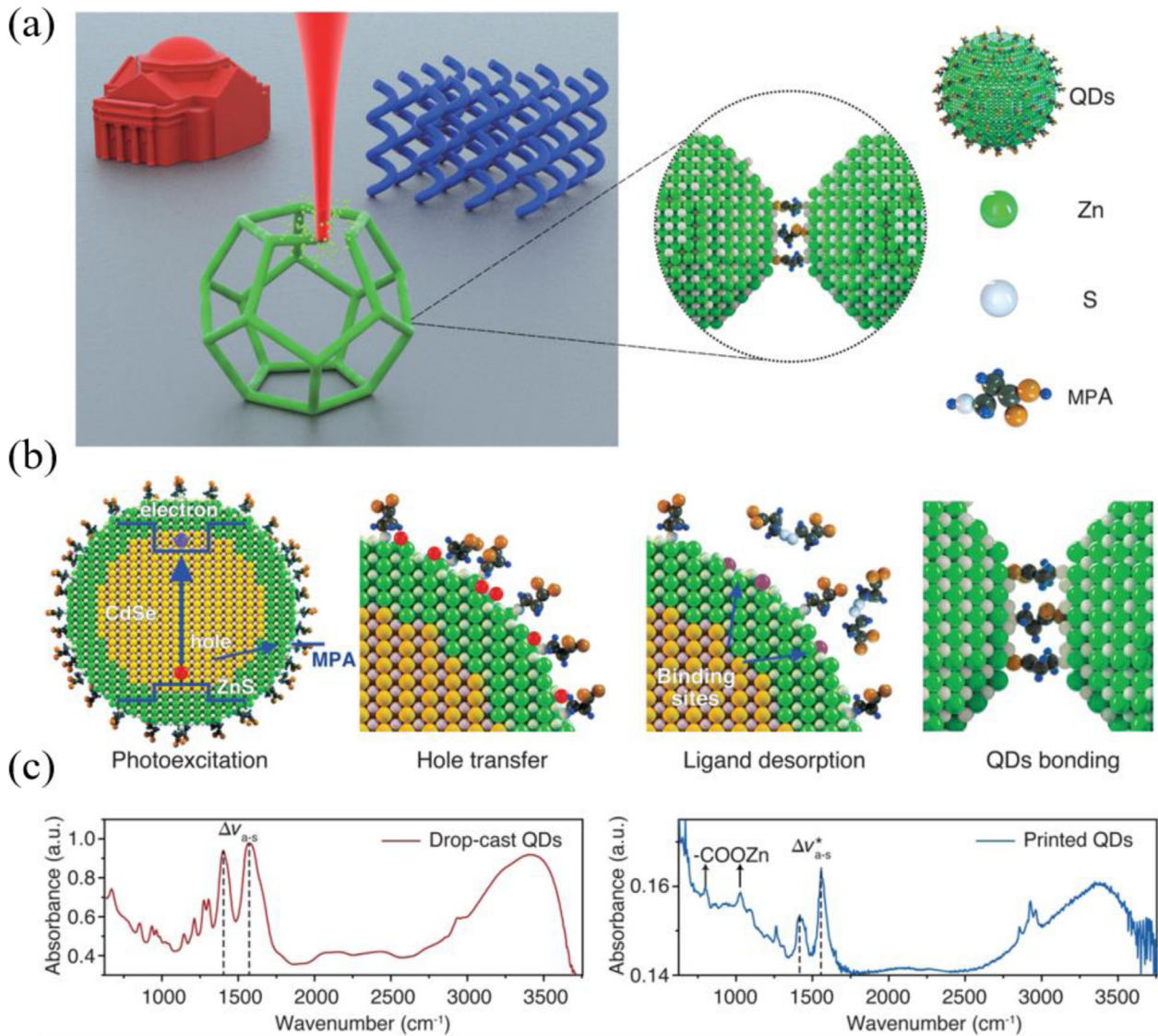


**Fig. 9.** 3D nanoprining of semiconductor quantum dots, (a) Schematic illustration showing 3D nanoprining of MPA-capped CdSe/ZnS QDs using PEB, (b) Schematic illustration showing the underlying mechanism of PEB, (c) FTIR spectra of the drop-cast QDs and printed structure. (reprinted with permission from Ref. [78]).

In the domain of metal component manufacturing, LPBF and LMD represent complementary approaches, with the former excelling in precision and geometric complexity, and the latter offering advantages in build size and production efficiency. VPP technologies remain unparalleled for high-precision fabrication of non-metallic materials and is advancing toward multi-material capability, high-speed printing, and volumetric additive manufacturing. Concurrently, LDW addresses the unique challenges associated with the additive manufacturing of functional nanostructures. For technology selection, researchers should first define the target material, key performance indicators (including strength, accuracy, build rate, and functional requirements), and the geometric characteristics of parts. The final decision can be made by applying the guidelines aforementioned above in conjunction with technology selection maps

available in the following section, such as charts correlating power or energy density with material properties.

### 3 Selection of LDAM

Figure 11 depicts the relationship between driving force, materials and AM technologies. The driving force can be categorized into several types, including light, electric arc, electron beam, heating, and pressure. Each category corresponds to specific AM technologies: for instance, electric arc-derived AM technology encompasses WAAM; electron beam-derived AM technology includes EBF and EBM; heating-derived AM technology comprises FDM and LOM; and pressure-derived AM technology covers DIW, 3DP, and IJP. As an essential component of AM, LDAM

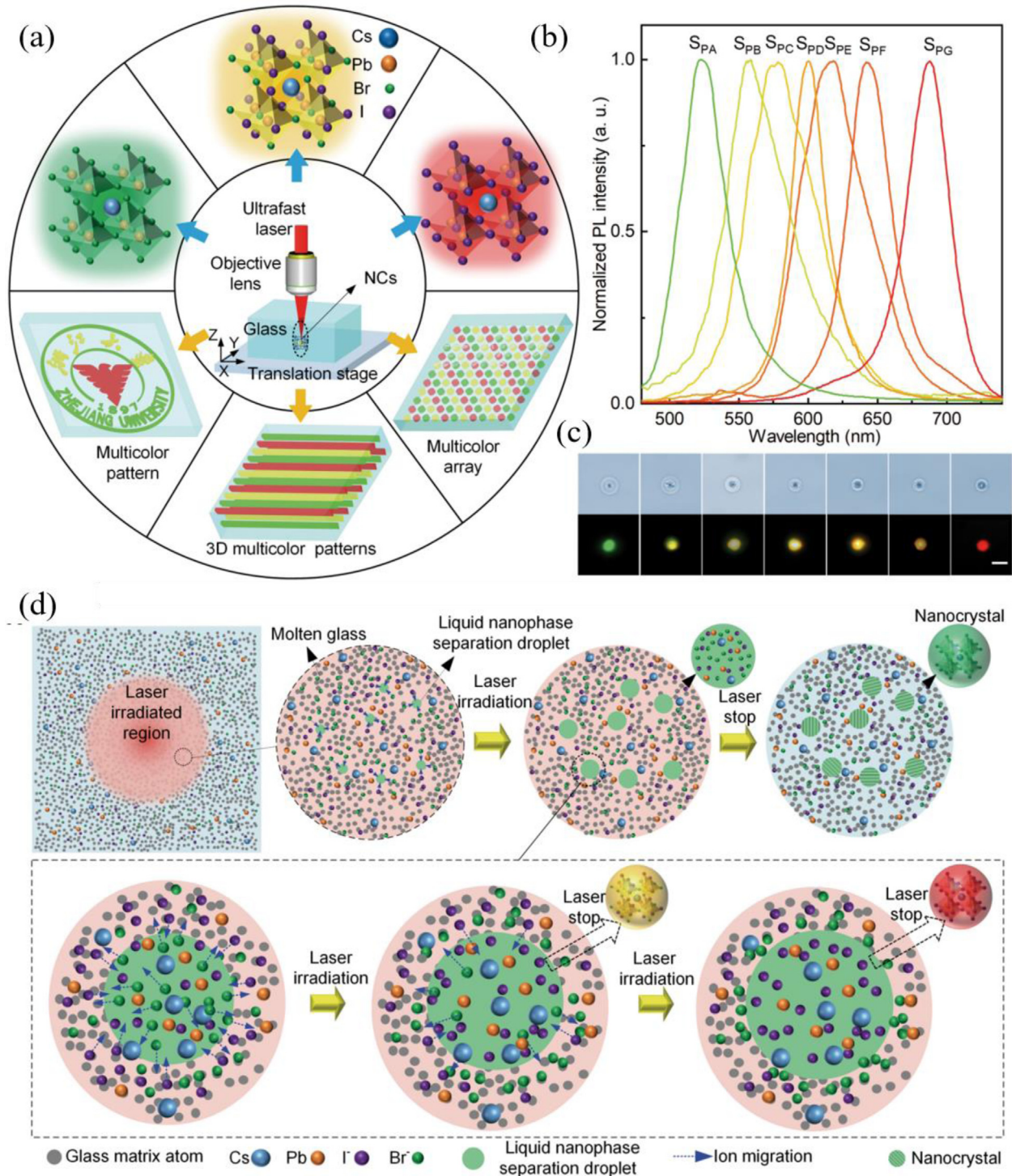


**Fig. 10.** Stable perovskite nanocrystals in glass by LDW technology. (a) Schematic illustration of direct lithography of colored PNCs and patterns, (b) PL spectra of CsPb(Br<sub>1-x</sub>I<sub>x</sub>)<sub>3</sub> PNCs written in one piece of glass, (c) Optical images (top) and PL mappings (bottom), (d) Schematic of ultrafast laser-induced liquid nanophase separation and formation of CsPb(Br<sub>1-x</sub>I<sub>x</sub>)<sub>3</sub> NCs. (reprinted with permission from Ref. [79]).

technologies encompass a variety of techniques, such as SLM, SLS, SLA, DLP, and CLIP. These technologies enable the production of parts in diverse materials, including SLM for metal and composite components,

and DLP for polymers, inorganic materials, and composites. This highlights the comprehensive and adaptable nature of each technology, underscoring substantial contributions to numerous fields.

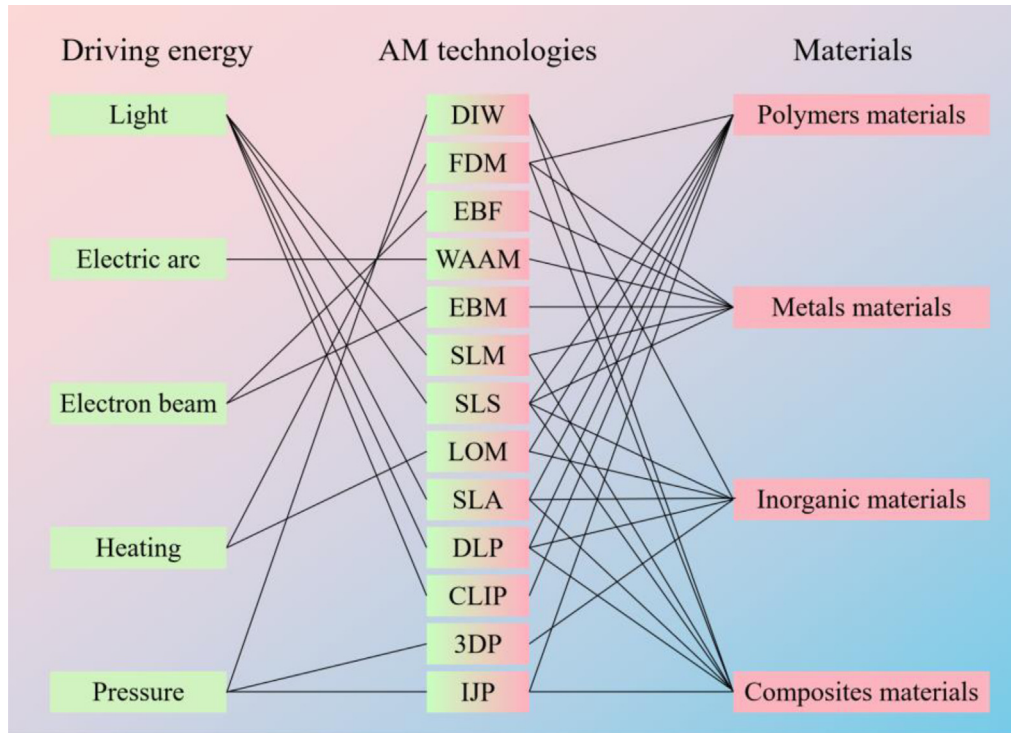


**Fig. 11.** The relationship of driving force, materials and AM technologies.

As previously mentioned, a variety of LDAM technologies have emerged, such as LMD, SLM, SLS, SLA, and DLP. These technologies are developed based on the principles of light properties and material characteristics. Their emergence represents a significant advancement in the field of AM, offering a promising solution to the rising demand for personalized parts fabricated from metals, ceramics, polymers, and composites. To facilitate the selection of an appropriate technology, we have statistically plotted the relationships between power and power density, power and energy density, along with material distributions for the relevant technologies. Researchers can thereby select the most suitable technology for the fabrication and production of the desired parts based on the corresponding data and the material-technology correspondence illustrated in [Figure 11](#).

As illustrated in [Figure 12](#), the power and power density required for the production of dense metal parts exceeds 50 W and  $10^4$  W/cm<sup>2</sup>, respectively. Similarly, the power and energy density should exceed 50W and  $10^3$  J/cm<sup>3</sup>, respectively. To obtain 3D-printed polymers with superior quality, the power and power density must fall within the ranges of 0.1–50 W and 0.001– $10^5$  W/cm<sup>2</sup>, respectively, while the power and energy density should be within the ranges of 0.1–50 W and 0.001– $10^3$  J/cm<sup>3</sup>, respectively. The range of ceramics is broader than that of polymers, as the ceramics are frequently prepared in conjunction with the polymers. Composites constitute a more expansive system, and a more precise range is determined based on the specific material system; However, the ranges presented in the review are applicable to all composite materials. As illustrated in [Figure 12](#), three primary options for AM

titanium alloys are available: SLM, LMD, and SLS. Considering density requirements of the parts, SLM and LMD may be more appropriate. Both SLM and LMD technologies enable the fabrication of high-density titanium alloys; SLM can produce finer parts, while LMD offers advantages in molding efficiency. Consequently, the final decision on which technology to utilize depends on the required part fineness and the equipment available.

## 4 Summary and prospects

### 4.1 Summary

The preceding sections presented a comprehensive analysis of the advancements and challenges encountered in four LDAM technologies: LPBF, LMD, VPP, and LDW. This section primarily serves to synthesize the preceding discussion, with the objective of consolidating pertinent insights for the benefit of the reader. Based on the literature referred in this review, research activity in the field of LPBF and VPP AM technologies is more extensive, whereas that in LMD and LDW is comparatively less prominent. Tendency uncovered from [Tables 1–4](#) suggests that there are still significant scientific and technological challenges to be addressed in the field of AM technology. Additionally, it also expounds that new printing methods, new materials, and high performance are the focal researches points, with other research concentrating on the optimization and enhancement of existing AM technologies or materials. In essence, these studies are all focused on the challenges and obstacles encountered in the field of AM.

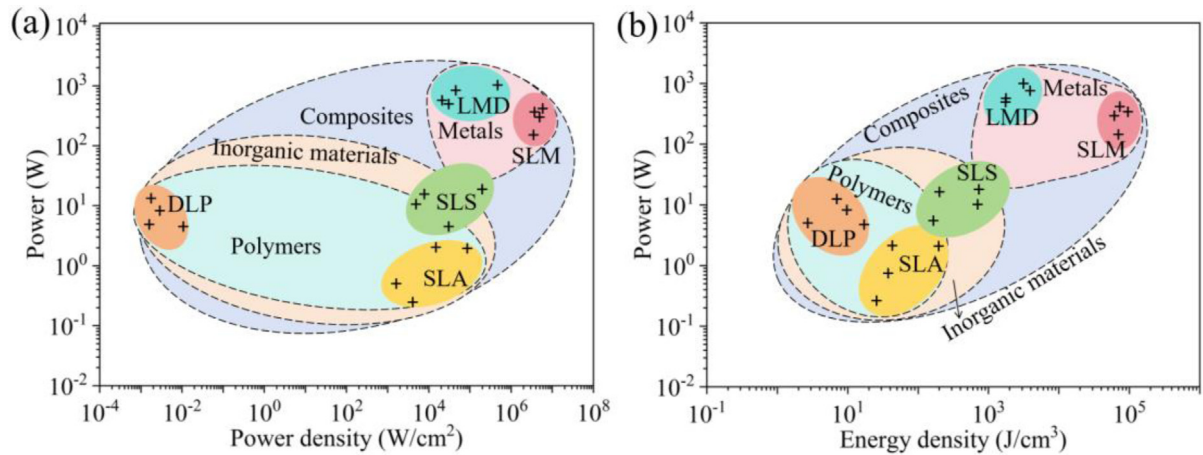


**Fig. 12.** The relationships between power and power density, and between power and energy density, along with the material distributions of the relevant technologies, SLA [81–83], DLP [47,84–86], SLS [87–89], SLM [29,31,33,90], LMD [32,38,40,41].

To address the current challenges in LPBF technology, researchers have conducted studies and proposed solutions from different perspectives. Defect control remains a core issue in the LPBF process, with ongoing research focusing on defect detection and characterization, particularly utilizing high-speed synchrotron X-ray imaging. Currently, process optimization and the introduction of external fields such as magnetic fields are effective strategies and methods to control defects. Additionally, the methods and materials currently employed in AM technology are insufficient to meet the demands of more practical applications. Consequently, a common approach involves leveraging existing materials to enhance overall performance through specific methods. Notably, the mechanical properties of 3D-printed materials, especially fatigue properties, are inadequate as well. Excitingly, the microstructure can be regulated by via targeted methods to improve these properties, as well as by structural and material design. Nonetheless, numerous challenges persist in LPBF technology, including lack of more effective strategies for defect control, deficiency in performance, inadequate AM efficiency, and insufficient the material system. It is widely anticipated that as these challenges are progressively addressed, LPBF will assume an increasingly significant role in material design and the manufacturing of high-performance components.

LMD provides significant advantages in near-net shape molding, particularly for the additive manufacturing of large components. However, the technology also presents significant challenges, particularly the scarcity of adequate novel and high-performance materials. In response, researchers have developed new materials tailored for the LMD process, combining process optimization and microstructure modulation. Excitingly, the construction of multi-material structures is feasible through the utilization of LMD platforms in a single manufacturing process. The capacity to customize the properties of materials at distinct locations represents a potentially transformative technology in the forthcoming years. The LMD process offers the flexibility in employing either individual materials or powder mixtures of different materials, enabling the precise control over the properties of each layer and region.

Therefore, the inherent flexibility and distinctive capabilities of LMD technology offer a promising outlook for its advancement.

Renowned for its high precision, VPP technology, encompassing distinctive techniques such as SLA, DLP, TPP and VAM, holds promising application prospects in fields including healthcare, mold manufacturing, aerospace, and automotive industries. The materials utilized in the SLA process are unrecyclable, and ongoing challenges, such as the design and synthesis of recyclable photosensitive resin materials, remain. Consequently, optimizing existing technologies and designing new materials constitute crucial steps in addressing the limitations of SLA process. The advent of DLP technology has enabled the low-cost fabrication of materials and parts at a faster speed, while also facilitating the production of components that are traditionally difficult to manufacture. Despite considerable progress, the future development of DLP technology still faces challenges such as limited performance and diversity of printable materials. Future research will therefore focus on overcoming these limitations through targeted technological advancements and methodological innovation. TPP technology is distinguished by its high precision and provides unparalleled advantages in AM and the fabrication of micro- and nano-devices. Furthermore, TPP is indispensable for the development of novel materials and technologies, while the manufacturing rate of AM remains a major limitation for its large-scale adoption. Therefore, future efforts aim to enhance fabrication efficiency while maintaining accuracy, such as through the utilization of metalens-generated focal spot array. VAM technology is currently constrained by limitations in speed, geometry, and surface quality. In response, novel VAM techniques have been designed and developed to address these issues, such as through the implementation of a novel light source mode. It is anticipated that future improvements in the accuracy, speed, and quality of AM will continue to be a significant and mainstream area of focus.

LDW technology, with its extremely high resolution, offers significant advantages in the fabrication of nano-materials and nanostructures, as it enables the creation of

nanostructures that are unattainable with conventional fabrication techniques. Moreover, it can create novel materials and structures within existing materials, such as glass, thereby eliminating the need for subsequent encapsulation and markedly enhancing device longevity. However, the primary obstacle to the wider implementation of LDW technology is its low productivity, as the writing speeds—currently on the order of mm/s—is insufficient for producing the macroscopic components for practical applications. To address this limitation, a combination of process development and the use of new high-performance materials is likely to prove an effective approach.

## 4.2 Future prospects

While each technology advances independently, shared interdisciplinary challenges and convergence trends are becoming increasingly prominent. A key frontier is the integration of functionalities, such as fabricating structurally robust components with embedded sensors (via LDW or VPP) or electrical pathways. Furthermore, the drive for multi-material AM is evident across all technologies, spanning from functionally graded metals in LMD to multi-material electronics in VPP. Additionally, the process monitoring and closed-loop control, pioneered in LPBF with high-speed imaging, are now essential for all light-derived additive manufacturing to ensure reliability and reproducibility. More importantly, the utilization of machine learning and digital twins is poised to accelerate materials discovery and process optimization across the board.

The Artificial Intelligence (AI), encompassing machine learning (ML) and its subset deep learning (DL), is poised to fundamentally promote light/laser-derived AM technology such as VPP and LPBF [91]. For example, Ren *et al.* employed machine learning to correlate the easily obtainable real-time thermal signals with the difficult-to-observe internal dynamics of the keyhole, particularly the pore-generating perturbative oscillations [27]. This connection enables the construction of a detection system that supports real-time prediction of pore generation events with extremely high accuracy and temporal resolution. Another key direction involves leveraging advanced ML and DL algorithms for the real-time, closed-loop optimization of critical process parameters, such as laser power, scan speed, and layer thickness [92]. In the future, AI will play an important role in design and process optimization, quality control and defect detection, predictive maintenance, materials development, process monitoring and control, as well as supply chain and workflow optimization [93].

## 5 Conclusions

In summary, this review has systematically examined the significant advances, persistent challenges, and future prospects of the four LDAM technologies: LPBF, LMD, VPP, and LDW. Each technology demonstrates unique capabilities, ranging from fabricating high-performance metal alloys to producing intricate micro-scale structures and functional materials. Despite remarkable progress,

challenges remain, including defect control in LPBF, material limitations in LMD, and the speed-resolution trade-off in VPP and LDW, which are pivotal objects for ongoing research. The future of LDAM lies in the intelligent integration of these technologies, the development of multi-material AM, and the employment of AI-driven process monitoring and closed-loop control. As these innovations converge, LDAM is poised to transform digital designs into complex, high-performance functional components with unprecedented efficiency and precision, further revolutionizing manufacturing across aerospace, medical, and electronics sectors.

## Funding

This work was supported by the National Key Research and Development Program of China (2024YFB3816500), National Natural Science Foundation of China (No. 52035014 and 52203203) and Zhejiang Provincial Natural Science Foundation of China (LQ24E050018).

## Conflicts of interest

The authors declare that they have no known competing financial interests or personal relationships that could have appeared to influence the work reported in this paper.

## Data availability statement

All data included in this study are available upon request by contact with the corresponding author.

## Author contribution statement

Chaoqian Zhao: Conceptualization, Writing—original draft, Resources, Validation, Funding acquisition. Defu Liu: Resources and Methodology. Jiawei Zhou: Methodology. Yong Hu and Gang Dong: Methodology and Funding acquisition. Zexin Yu, Liang Wang and Qunli Zhang: Writing—review & editing. Jianhua Yao: Conceptualization, Supervision, Writing—review & editing, Funding acquisition.

## References

1. Y. Lakhdar, C. Tuck, J. Binner, A. Terry, R. Goodridge, Additive manufacturing of advanced ceramic materials, *Prog. Mater. Sci.* **116** (2021) 100736
2. A.A. Elhadad, A. Rosa-Sainz, R. Canete, E. Peralta, B. Begines, M. Balbuena, A. Alcudia, Y. Torres, Applications and multidisciplinary perspective on 3D printing techniques: recent developments and future trends, *Mater. Sci. Eng.: R: Reports* **156** (2023) 100760
3. X. Cui, J. Zhang, Y. Qian, S. Chang, B.J. Allardyce, R. Rajkhowa, H. Wang, K. Zhang, 3D printing strategies for precise and functional assembly of silk-based biomaterials, *Engineering* **34** (2024) 92–108
4. A. Christensen, Chapter 1 - An abbreviated history of medical 3D printing, in: N. Wake (Ed.), *3D Printing for the Radiologist*, Elsevier, 2022, pp. 1-10

5. A. Su, S.J. Al'Aref, Chapter 1 - History of 3D printing, in: S.J. Al'Aref, B. Mosadegh, S. Dunham, J.K. Min (Eds.), 3D Printing Applications in Cardiovascular Medicine, Academic Press, Boston, 2018, pp. 1-10
6. Q. Yan, H. Dong, J. Su, J. Han, B. Song, Q. Wei, Y. Shi, A review of 3D printing technology for medical applications, *Engineering* **4** (2018) 729–742
7. X.N. Zhang, Q. Zheng, Z.L. Wu, Recent advances in 3D printing of tough hydrogels: a review, *Compos. Part B: Eng.* **238** (2022) 109895
8. G. Liu, X. Zhang, X. Chen, Y. He, L. Cheng, M. Huo, J. Yin, F. Hao, S. Chen, P. Wang, S. Yi, L. Wan, Z. Mao, Z. Chen, X. Wang, Z. Cao, J. Lu, Additive manufacturing of structural materials, *Mater. Sci. Eng.: R: Reports* **145** (2021) 100596
9. R.P. Chaudhary, C. Parameswaran, M. Idrees, A.S. Rasaki, C. Liu, Z. Chen, P. Colombo, Additive manufacturing of polymer-derived ceramics: materials, technologies, properties and potential applications, *Prog. Mater. Sci.* **128** (2022) 100969
10. H.W. Tan, Y.Y.C. Choong, C.N. Kuo, H.Y. Low, C.K. Chua, 3D printed electronics: Processes, materials and future trends, *Prog. Mater. Sci.* **127** (2022) 100945
11. A. Bandyopadhyay, B. Heer, Additive manufacturing of multi-material structures, *Mater. Sci. Eng.: R: Reports* **129** (2018) 1–16
12. A. Bandyopadhyay, K.D. Traxel, S. Bose, Nature-inspired materials and structures using 3D Printing, *Mater. Sci. Eng.: R: Reports* **145** (2021) 100609
13. X.-Y. Ding, Y.-C. Fu, B. Li, S. Lin, L.-M. Luo, Y.-C. Wu, J.-H. Yao, Microstructure and mechanical properties of Al<sub>2</sub>O<sub>3</sub> dispersion strengthened Cu by laser in-situ aluminum thermal reduction processing, *Mater. Des.* **258** (2025) 114547
14. K. Khan, M.I. Hussain, A.K. Tareen, A. Asghar, M. Hamza, Z. Chen, Advances in vat photopolymerization 3D printing: multifunctional materials, process innovations, and emerging applications, *Mater. Sci. Eng.: R: Reports* **167** (2026) 101120
15. Y. Yang, R. Jiang, C. Han, J. Chen, H. Li, Y. Wang, J. Tang, H. Zhou, W. Hu, B. Zheng, Z. Liu, C. Song, D. Wang, *Frontiers in laser additive manufacturing technology*, *Addit. Manuf. Front.* **3** (2024) 200160
16. E. Stratakis, J. Bonse, J. Heitz, J. Siegel, G.D. Tsibidis, E. Skoulas, A. Papadopoulos, A. Mimidis, A.C. Joel, P. Comanns, J. Krüger, C. Florian, Y. Fuentes-Edfuf, J. Solis, W. Baumgartner, Laser engineering of biomimetic surfaces, *Mater. Sci. Eng.: R: Reports* **141** (2020) 100562
17. H. Wang, D. Deng, Z. Zhai, Y. Yao, Laser-processed functional surface structures for multi-functional applications-a review, *J. Manuf. Process.* **116** (2024) 247–283
18. R. Huang, H. Guo, Z. Gu, Y. Ling, Advances in laser processed material of soft sensing and soft actuation, *Mater. Today Commun.* **37** (2023) 107187
19. A. S., D.W.R. D., A. Jain, J. Kandasamy, M. Singhal, Laser processing techniques for surface property enhancement: focus on material advancement, *Surf. Interfaces* **42** (2023) 103293
20. H. Sun, B. Zou, X. Wang, W. Chen, G. Zhang, T. Quan, C. Huang, Advancements in multi-material additive manufacturing of advanced ceramics: a review of strategies, techniques and equipment, *Mater. Chem. Phys.* **319** (2024) 129337
21. C. Zhao, N.D. Parab, X.X. Li, K. Fezzaa, W.D. Tan, A.D. Rollett, T. Sun, Critical instability at moving keyhole tip generates porosity in laser melting, *Science* **370** (2020) 1080–1086
22. S.E. Alkhatib, T.B. Sercombe, High strain-rate response of additively manufactured light metal alloys, *Mater. Des.* **217** (2022) 110664
23. B. Soundararajan, D. Sofia, D. Barletta, M. Poletto, Review on modeling techniques for powder bed fusion processes based on physical principles, *Addit. Manuf.* **47** (2021) 102336
24. S.L. Sing, S. Huang, G.D. Goh, G.L. Goh, C.F. Tey, J.H.K. Tan, W.Y. Yeong, Emerging metallic systems for additive manufacturing: in-situ alloying and multi-metal processing in laser powder bed fusion, *Prog. Mater. Sci.* **119** (2021) 100795
25. S.A. Khairallah, A.A. Martin, J.R.I. Lee, G. Guss, N.P. Calta, J.A. Hammons, M.H. Nielsen, K. Chaput, E. Schwalbach, M.N. Shah, M.G. Chapman, T.M. Willey, A. M. Rubenchik, A.T. Anderson, Y.M. Wang, M.J. Matthews, W.E. King, Controlling interdependent meso-nanosecond dynamics and defect generation in metal 3D printing, *Science* **368** (2020) 660–665
26. R. Cunningham, C. Zhao, N. Parab, C. Kantzos, J. Pauza, K. Fezzaa, T. Sun, A.D. Rollett, Keyhole threshold and morphology in laser melting revealed by ultrahigh-speed x-ray imaging, *Science* **363** (2019) 849–852
27. Z.S. Ren, L. Gao, S.J. Clark, K. Fezzaa, P. Shevchenko, A. Choi, W. Everhart, A.D. Rollett, L.Y. Chen, T. Sun, Machine learning-aided real-time detection of keyhole pore generation in laser powder bed fusion, *Science* **379** (2023) 89–93
28. X. Fan, T.G. Fleming, S.J. Clark, K. Fezzaa, A.C.M. Getley, S. Marussi, H. Wang, C.L.A. Leung, A. Kao, P.D. Lee, Magnetic modulation of keyhole instability during laser welding and additive manufacturing, *Science* **387** (2025) 864–869
29. T.L. Zhang, Z.H. Huang, T. Yang, H.J. Kong, J.H. Luan, A.D. Wang, D. Wang, W. Kuo, Y.Z. Wang, C.T. Liu, In situ design of advanced titanium alloy with concentration modulations by additive manufacturing, *Science* **374** (2021) 478–482
30. T.M. Smith, C.A. Kantzos, N.A. Zarkevich, B.J. Harder, M. Heczko, P.R. Gradl, A.C. Thompson, M.J. Mills, T.P. Gabb, J.W. Lawson, A 3D printable alloy designed for extreme environments, *Nature* **617** (2023) 513–518
31. J.Q. Zhang, M.J. Birmingham, J. Otte, Y.G. Liu, Z.Y. Hou, N. Yang, Y. Yin, M. Bayat, W.K. Lin, X.X. Huang, D.H. StJohn, M.S. Dargusch, Ultrauniform, strong, and ductile 3D-printed titanium alloy through bifunctional alloy design, *Science* **383** (2024) 639–645
32. J. Ren, Y. Zhang, D.X. Zhao, Y. Chen, S. Guan, Y.F. Liu, L. Liu, S.Y. Peng, F.Y. Kong, J.D. Poplawsky, G.H. Gao, T. Voisin, K. An, Y.M. Wang, K.Y. Xie, T. Zhu, W. Chen, Strong yet ductile nanolamellar high-entropy alloys by additive manufacturing, *Nature* **608** (2022) 62–68
33. Z. Qu, Z.J. Zhang, R. Liu, L. Xu, Y.N. Zhang, X.T. Li, Z.K. Zhao, Q.Q. Duan, S.G. Wang, S.J. Li, Y.J. Ma, X.H. Shao, R. Yang, J. Eckert, R.O. Ritchie, Z.F. Zhang, High fatigue resistance in a titanium alloy via near-void-free 3D printing, *Nature* **626** (2024) 999–1004
34. Y.F. Wang, L.C. Li, D. Hofmann, J.E. Andrade, C. Daraio, Structured fabrics with tunable mechanical properties, *Nature* **596** (2021) 238–243
35. D. Svetlizky, M. Das, B. Zheng, A.L. Vyatskikh, S. Bose, A. Bandyopadhyay, J.M. Schoenung, E.J. Lavernia, N. Eliaz, Directed energy deposition (DED) additive manufacturing: physical characteristics, defects, challenges and applications, *Mater. Today* **49** (2021) 271–295

36. A. Azarniya, X.G. Colera, M.J. Mirzaali, S. Sovizi, F. Bartolomeu, M.k. St Weglowski, W.W. Wits, C.Y. Yap, J. Ahn, G. Miranda, F.S. Silva, H.R. Madaah Hosseini, S. Ramakrishna, A.A. Zadpoor, Additive manufacturing of Ti–6Al–4V parts through laser metal deposition (LMD): process, microstructure, and mechanical properties, *J. Alloys Compd.* **804** (2019) 163–191
37. P. Ghosal, M.C. Majumder, A. Chattopadhyay, Study on direct laser metal deposition, *Mater. Today: Proc.* **5** (2018) 12509–12518
38. H.L. Hou, E. Simsek, T. Ma, N.S. Johnson, S.X. Qian, C. Cissé, D. Stasak, N. Al Hasan, L. Zhou, Y.H. Hwang, R. Radermacher, V.I. Levitas, M.J. Kramer, M.A. Zaem, A.P. Stebner, R.T. Ott, J. Cui, I. Takeuchi, Fatigue-resistant high-performance elastocaloric materials made by additive manufacturing, *Science* **366** (2019) 1116–1121
39. T.T. Song, Z.B. Chen, X.Y. Cui, S.L. Lu, H.S. Chen, H. Wang, T. Dong, B.L. Qin, K.C. Chan, M. Brandt, X.Z. Liao, S.P. Ringer, M. Qian, Strong and ductile titanium-oxygen-iron alloys by additive manufacturing, *Nature* **618** (2023) 63–68
40. P. Kürnsteiner, M.B. Wilms, A. Weisheit, B. Gault, E.A. Jäggle, D. Raabe, High-strength Damascus steel by additive manufacturing, *Nature* **582** (2020) 515–519
41. D.Y. Zhang, D. Qiu, M.A. Gibson, Y.F. Zheng, H.L. Fraser, D.H. StJohn, M.A. Easton, Additive manufacturing of ultrafine-grained high-strength titanium alloys, *Nature* **576** (2019) 91–95
42. F. Zhang, L. Zhu, Z. Li, S. Wang, J. Shi, W. Tang, N. Li, J. Yang, The recent development of vat photopolymerization: a review, *Addit. Manuf.* **48** (2021) 102423
43. A. Al Rashid, W. Ahmed, M.Y. Khalid, M. Koç, Vat photopolymerization of polymers and polymer composites: processes and applications, *Addit. Manuf.* **47** (2021) 102279
44. C. Zhao, T. Wang, J. Zhou, D. Liu, Y. Hu, L. Wang, Q. Zhang, Y. Zhu, J. Yao, Pulsed-switchable strategy and relative-pressure control optimizing multi-ceramics 3D printing integrated with laser-assisted curing, *Addit. Manuf.* **110** (2025) 104946
45. D. Chekkaramkodi, L. Jacob, M.S. C, R. Umer, H. Butt, Review of vat photopolymerization 3D printing of photonic devices, *Addit. Manuf.* **86** (2024) 104189
46. J. Herzberger, J.M. Serrine, C.B. Williams, T.E. Long, Polymer design for 3D printing elastomers: recent advances in structure, properties, and printing, *Prog. Polym. Sci.* **97** (2019) 101144
47. B. Grigoryan, S.J. Paulsen, D.C. Corbett, D.W. Sazer, C.L. Fortin, A.J. Zaita, P.T. Greenfield, N.J. Calafat, J.P. Gounley, A.H. Ta, F. Johansson, A. Randles, J.E. Rosenkrantz, J.D. Louis-Rosenberg, P.A. Galie, K.R. Stevens, J. S. Miller, Biomedicine multivascular networks and functional intravascular topologies within biocompatible hydrogels, *Science* **364** (2019) 458–464
48. T.O. Machado, C.J. Stubbs, V. Chiaradia, M.A. Alraddadi, A. Brandolese, J.C. Worch, A.P. Dove, A renewably sourced, circular photopolymer resin for additive manufacturing, *Nature* **629** (2024) 1069–1074
49. B. Yang, T. Ni, J. Wu, Z. Fang, K. Yang, B. He, X. Pu, G. Chen, C. Ni, D. Chen, Q. Zhao, W. Li, S. Li, H. Li, N. Zheng, T. Xie, Circular 3D printing of high-performance photopolymers through dissociative network design, *Science* **388** (2025) 170–175
50. H.C. Cui, D.S. Yao, R. Hensleigh, H.T. Lu, A. Calderon, Z.P. Xu, S. Davaria, Z. Wang, P. Mercier, P. Tarazaga, X.Y. Zheng, Design and printing of proprioceptive three-dimensional architected robotic metamaterials, *Science* **376** (2022) 1287–1293
51. C. Zhu, J.B. Jin, Z. Wang, Z.P. Xu, M.C. Folgueras, Y.X. Jiang, C.B. Uzundal, H.K.D. Le, F. Wang, X.Y. Zheng, P.D. Yang, Supramolecular assembly of blue and green halide perovskites with near-unity photoluminescence, *Science* **383** (2024) 86–93
52. M.A. Saccone, R.A. Gallivan, K. Narita, D.W. Yee, J.R. Greer, Additive manufacturing of micro-architected metals via hydrogel infusion, *Nature* **612** (2022) 685–690
53. D.A. Walker, J.L. Hedrick, C.A. Mirkin, Rapid, large-volume, thermally controlled 3D printing using a mobile liquid interface, *Science* **366** (2019) 360–364
54. A.J. Commisso, E.M. Nagel, M.T. Kiker, E.A. Recker, A. Bischoff, M.J. Holzmann, H.E. Fowler, M.N. Pham, C.P.H. Nguyen, E. Baca, H. Villanueva, N.T. Almada, K.S. Mason, C. Jolowsky, G. Suman, K.J. Fritzscheing, B. Kaehr, J.J. Schwartz, L.N. Appelhans, B.H. Jones, C.S. Sample, D.J. Roach, Z.A. Page, S.C. Leguizamon, Lithographic crystallinity regulation in additive fabrication of thermoplastics (CRAFT), *Science* **391** (2026) 511–516
55. J. Bauer, C. Crook, T. Baldacchini, A sinterless, low-temperature route to 3D print nanoscale optical-grade glass, *Science* **380** (2023) 960–966
56. F. Li, S.-F. Liu, W. Liu, Z.-W. Hou, J. Jiang, Z. Fu, S. Wang, Y. Si, S. Lu, H. Zhou, D. Liu, X. Tian, H. Qiu, Y. Yang, Z. Li, X. Li, L. Lin, H.-B. Sun, H. Zhang, J. Li, 3D printing of inorganic nanomaterials by photochemically bonding colloidal nanocrystals, *Science* **381** (2023) 1468–1474
57. S.K. Saha, D. Wang, V.H. Nguyen, Y.N. Chang, J.S. Oakdale, S.C. Chen, Scalable submicrometer additive manufacturing, *Science* **366** (2019) 105–109
58. S. Gu, C. Mao, A. Guell Izard, S. Sadana, D. Terrel-Perez, M. Mettry-Yassa, W. Choi, W. Zhou, H. Yan, Z. Zhou, T. Massey, A. Abelson, Y. Zhou, S. Huang, C. Daraio, T.U. Tumkur, J.A. Fan, X. Xia, 3D nanolithography with metalens arrays and spatially adaptive illumination, *Nature* **648** (2025) 591–599
59. S. Xu, X. Xia, Q. Yu, A. Parakh, S. Khan, E. Megidish, B. You, B. Hemmerling, A. Jayich, K. Beck, J. Biener, H. Häffner, 3D-printed micro ion trap technology for quantum information applications, *Nature* **645** (2025) 362–368
60. W. Zhou, S. Nadarajah, L. Li, A.G. Izard, H. Yan, A.K. Prachet, P. Patel, X. Xia, C. Daraio, 3D polycatenated architected materials, *Science* **387** (2025) 269–277
61. J.M. Kronenfeld, L. Rother, M.A. Saccone, M.T. Dulay, J.M. DeSimone, Roll-to-roll, high-resolution 3D printing of shape-specific particles, *Nature* **627** (2024) 306–312
62. J.R. Tumbleston, D. Shirvanyants, N. Ermoshkin, R. Januszewicz, A.R. Johnson, D. Kelly, K. Chen, R. Pinschmidt, J.P. Rolland, A. Ermoshkin, E.T. Samulski, J.M. DeSimone, Continuous liquid interface production of 3D objects, *Science* **347** (2015) 1349–1352
63. B.E. Kelly, I. Bhattacharya, H. Heidari, M. Shusteff, C.M. Spadaccini, H.K. Taylor, Volumetric additive manufacturing via tomographic reconstruction, *Science* **363** (2019) 1075–1079
64. S.N. Sanders, T.H. Schloemer, M.K. Gangishetty, D. Anderson, M. Seitz, A.O. Gallegos, R.C. Stokes, D.N. Congreve, Triplet fusion upconversion nanocapsules for volumetric 3D printing, *Nature* **604** (2022) 474–478

65. J.T. Toombs, M. Luitz, C.C. Cook, S. Jenne, C.C. Li, B.E. Rapp, F. Kotz-Helmer, H.K. Taylor, Volumetric additive manufacturing of silica glass with microscale computed axial lithography, *Science* **376** (2022) 308–312
66. M. Regehly, Y. Garmshausen, M. Reuter, N.F. König, E. Israel, D.P. Kelly, C.Y. Chou, K. Koch, B. Asfari, S. Hecht, Xolography for linear volumetric 3D printing, *Nature* **588** (2020) 620–624
67. S. Florczak, G. Größbacher, D. Ribezzi, A. Longoni, M. Gueye, E. Grandidier, J. Malda, R. Levato, Adaptive and context-aware volumetric printing, *Nature* **645** (2025) 108–114
68. X. Wang, Y. Ma, Y. Niu, B. Xiong, A. Zhang, G. Zhang, Y. Chen, W. Wei, L. Fang, J. Wu, Q. Dai, Sub-second volumetric 3D printing by synthesis of holographic light fields, *Nature* **650** (2026) 882–890
69. F. Han, S.Y. Gu, A. Klimas, N. Zhao, Y.X. Zhao, S.C. Chen, Three-dimensional nanofabrication via ultrafast laser patterning and kinetically regulated material assembly, *Science* **378** (2022) 1325–1331
70. T.J.K. Buchner, S. Rogler, S. Weirich, Y. Armati, B.G. Cangan, J. Ramos, S.T. Twiddy, D.M. Marini, A. Weber, D. Chen, G. Ellson, J. Jacob, W. Zengerle, D. Katalichenko, C. Keny, W. Matusik, R.K. Katzschmann, Vision-controlled jetting for composite systems and robots, *Nature* **623** (2023) 522–530
71. J. Li, C. Wu, P.K. Chu, M. Gelinsky, 3D printing of hydrogels: rational design strategies and emerging biomedical applications, *Mater. Sci. Eng.: R: Reports* **140** (2020) 100543
72. Z. Wang, W. Yang, Y. Qin, W. Liang, H. Yu, L. Liu, Digital micro-mirror device -based light curing technology and its biological applications, *Opt. Laser Technol.* **143** (2021) 107344
73. H.W. Gao, J. An, C.K. Chua, D. Bourell, C.N. Kuo, D.T.H. Tan, 3D printed optics and photonics: processes, materials and applications, *Mater. Today* **69** (2023) 107–132
74. Q. Thijssen, J. Toombs, C.C. Li, H. Taylor, S. Van Vlierberghe, From pixels to voxels: a mechanistic perspective on volumetric 3D-printing, *Prog. Polym. Sci.* **147** (2023) 101755
75. D.J. Whyte, E.H. Doeven, A. Sutti, A.Z. Kouzani, S.D. Adams, Volumetric additive manufacturing: a new frontier in layer-less 3D printing, *Addit. Manuf.* **84** (2024) 104094
76. A. Selimis, V. Mironov, M. Farsari, Direct laser writing: principles and materials for scaffold 3D printing, *Microelectron. Eng.* **132** (2015) 83–89
77. S. Wang, Z. Zhou, B. Li, C. Wang, Q. Liu, Progresses on new generation laser direct writing technique, *Mater. Today Nano* **16** (2021) 100142
78. S.F. Liu, Z.W. Hou, L.H. Lin, F. Li, Y. Zhao, X.Z. Li, H. Zhang, H.H. Fang, Z.C. Li, H.B. Sun, 3D nanoprinting of semiconductor quantum dots by photoexcitation-induced chemical bonding, *Science* **377** (2022) 1112–1116
79. K. Sun, D.Z. Tan, X.Y. Fang, X.T. Xia, D.J. Lin, J. Song, Y. H. Lin, Z.J. Liu, M. Gu, Y.Z. Yue, J.R. Qiu, Three-dimensional direct lithography of stable perovskite nanocrystals in glass, *Science* **375** (2022) 307.
80. X.Y. Xu, T.X. Wang, P.C. Chen, C. Zhou, J.A. Ma, D.Z. Wei, H.J. Wang, B. Niu, X.Y. Fang, D. Wu, S.N. Zhu, M. Gu, M. Xiao, Y. Zhang, Femtosecond laser writing of lithium niobate ferroelectric nanodomains, *Nature* **609** (2022) 496–501
81. Y.J. Kim, H.N. Kim, D.Y. Kim, A study on effects of curing and machining conditions in post-processing of SLA additive manufactured polymer, *J. Manuf. Process.* **119** (2024) 511–519
82. Y. Yu, B. Zou, X. Wang, C. Huang, Rheological behavior and curing deformation of paste containing 85 wt% Al<sub>2</sub>O<sub>3</sub> ceramic during SLA-3D printing, *Ceram. Int.* **48** (2022) 24560–24570
83. Y. Nian, S. Wan, M. Avcar, R. Yue, M. Li, 3D printing functionally graded metamaterial structure: design, fabrication, reinforcement, optimization, *Int. J. Mech. Sci.* **258** (2023) 108580
84. S. Zhang, I.A. Sutejo, C.W. Gal, Y.-J. Choi, H.-N. Kim, Y.-J. Park, H.-s. Yun, Fabrication of highly transparent yttria by DLP-based additive manufacturing, *J. Eur. Ceram. Soc.* **44** (2024) 6037–6046
85. G. Zhu, M. Liu, S. Weng, G. Zhang, Y. Hu, Z. Kou, C. Bo, L. Hu, S. Wu, Y. Zhou, Dye-free and reprintable multi-color DLP 3D printing using ZnCl<sub>2</sub>-based polymerizable deep eutectic solvents and type I photoinitiators, *Chem. Eng. J.* **472** (2023) 144987
86. X. Zhang, Y. Rong, H. Li, J. Fei, X. Huang, Q. Bao, J. An, High tensile properties, wide temperature tolerance, and DLP-printable eutectogels for microarrays wearable strain sensors, *Chem. Eng. J.* **481** (2024) 149004
87. K. Deng, H. Wu, Y. Li, J. Jiang, Z. Yang, R. Zhang, S. Liu, B. Chao, W. Fu, M. Wang, Porous NFG/SiC<sub>n</sub>w composites fabricated by SLS for structural load-bearing and functionally integrated electromagnetic absorption, *Ceram. Int.* **49** (2023) 28547–28559
88. Y. Yang, T. Zeng, Z. Liang, D. Li, G. Xu, X. Wang, S. Cheng, Effect of graphite content on the microstructure and mechanical properties of SLS-based RB-SiC ceramics, *Ceram. Int.* **50** (2024) 22858–22864
89. M.K. Razaviye, R.A. Tafti, M. Khajehmohammadi, An investigation on mechanical properties of PA12 parts produced by a SLS 3D printer: an experimental approach, *CIRP J. Manuf. Sci. Technol.* **38** (2022) 760–768
90. J. Chen, X. Ding, J. Wang, Z. Xie, S. Wang, Corrosion behavior, metal ions release and wear resistance of TiN coating deposited on SLM CoCrMo alloy by magnetron sputtering, *J. Alloys Compd.* (2024) 175318.
91. Y. Du, T. Mukherjee, R. Li, Z. Hou, S. Dutta, C.B. Arnold, A. Elwany, S. Kung, J. Tang, T. DebRoy, A review of deep learning in metal additive manufacturing: impact on process, structure, and properties, *Prog. Mater. Sci.* **157** (2026) 101587
92. T. Özel, Deep learning-based applications in metal additive manufacturing processes: challenges and opportunities—a review, *Int. J. Lightweight Mater. Manuf.* **8** (2025) 453–468
93. M. Soori, F.K.G. Jough, R. Dastres, B. Arezoo, Additive manufacturing modification by artificial intelligence, machine learning, and deep learning: a review, *Addit. Manuf. Front.* **4** (2025) 200198